A THEORETICAL AND EXPERIMENTAL STUDY OF SODIUM
ION TRANSFER IN BLOOD VESSEL WALLS

Dissertation for the Degree of Ph. D.
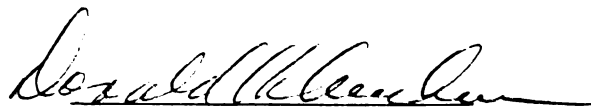MICHIGAN STATE UNIVERSITY
WON HONG LEE
1975

This is to certify that the

thesis entitled

A THEORETICAL AND EXPERIMENTAL STUDY OF SODIUM
ION TRANSFER IN BLOOD VESSEL WALLS

presented by

WON HONG LEE

has been accepted towards fulfillment
of the requirements for

_____Ph.D._____ degree in _Chemical_
~~Engineering~~

Donald K. Anderson

Major professor

Date___September 19, 1975___

O-7639

ABSTRACT

A THEORETICAL AND EXPERIMENTAL STUDY OF SODIUM
ION TRANSFER IN BLOOD VESSEL WALLS

By

Won Hong Lee

Transfer of ions within the walls of blood vessels plays an
important role in the contractile process of smooth muscle cells
located in those walls. This effect is in large part mediated
through the cell potential; depolarization leads to contraction and
hyperpolarization to relaxation. The cell potential in turn is
maintained by active transport of sodium ions out of and potassium
ions into the cells. In the steady state, this active transport is
balanced by diffusive transport in the opposite direction under the
influence of electrochemical driving forces.

The kinetics of transport of sodium ions in arterial walls
(branches of canine femoral artery) were studied both theoretically
and experimentally. A tracer washout technique was developed to
permit the use in the experiments of sections of artery rather than
strips cut from arteries as in previous studies. The artery sections
were mounted on stainless steel rods with only the outer surface of
the tissue being washed. In this manner, tension was maintained in
the wall to more closely approximate the conditions of intact tissue.
The artery mounted on the rod was incubated in physiologic Ringer's

solution tagged with Na^{22} and washed with a tag free solution. The total radioactivity remaining in the tissue was measured as a function of time with a scintillation detector crystal. The experimental washout data were then analyzed based on a mathematical model developed in this work. The model takes into account diffusion in the extracellular space and transport across the cell membrances by both passive and active mechanisms.

Values were obtained at 37°C for the diffusion coefficient to the sodium ion in the extracellular space (8.33×10^{-6} cm^2/sec), the membrane permeability to sodium ion (0.6×10^{-8} cm/sec), the rate of active transport of sodium ions through the cell membrane (2.09×10^{-9} mEq/cm^2sec), and the intracellular sodium concentration (18.7 mEq/1) under normal conditions.

A study of the effects on Na^{22} transport of lowering $[K^+]_e$ indicates that $[Na^+]_i$ increases as $[K^+]_e$ is decreased, while the membrane permeability remains essentially constant. There was no significant decrease in the rate of active transport with decreased $[K^+]_e$. However, that result must be questioned since one would expect low $[K^+]_e$ to inhibit the Na^+-K^+ pump and thus active extrusion of sodium.

When the temperature was lowered to 21.2°C, the diffusion coefficient (6.88×10^{-6} cm^2/sec), membrane permeability (0.52×10^{-8} cm/sec), and rate of active transport (1.52×10^{-9} mEq/cm^2sec) decreased and the intracellular sodium concentration (27.5 mEq/1) increased.

Generally, the results obtained from this study are consistent with the hypothesis that an electrogenic Na^+-K^+ pump plays an important role in maintaining the cell potential, indicating that the changes in potential are not mediated through changes in permeability when $[K^+]_e$ are altered. The results also indicate that when using washout techniques to study ion transport, the tissue must be incubated in a solution of the same ion composition as the washing solution to insure a steady state.

A THEORETICAL AND EXPERIMENTAL STUDY OF SODIUM

ION TRANSFER IN BLOOD VESSEL WALLS

By

Won Hong Lee

A DISSERTATION

Submitted to
Michigan State University
in partial fulfillment of the requirements
for the degree of

DOCTOR OF PHILOSOPHY

Department of Chemical Engineering

1975

To my parents

ACKNOWLEDGMENTS

TABLE OF CONTENTS

LIST OF TABLES

LIST OF FIGURES

NOMENCLATURE

Symbol	Definition
a	chemical activity; cell membrane area per unit cell volume; inside radius of tissue
A	cell surface area; element of eigen vector
b	outside radius of tissue
B	proportionality constant
C	concentration
Ca	calcium
Cl	chloride
d	membrane thickness
D	diffusion coefficient
E	electrical potential
F	Faraday
j	ion flux
K	transfer rate constant; potassium
L	length of tissue
M	number of moles diffused out of tissue
Mg	magnesium
n	molar flux
N	radioactivity; integration constant
Na	sodium
P	membrane permeability
R	gas constant

Symbol	Definition
r	Na to K exchange ratio of pump
S	rate of active transport of sodium ions across the cell membrane
t	time
T	absolute temperature
u	ion mobility
v	ion mobility
V	tissue volume
z	ion valence
α	eigenvalue of the $[\lambda]$ matrix
β	partition coefficient
ϵ	volume fraction
μ	chemical potential
λ	turn over rate

Subscripts

a	active
d	membrane thickness
dif	diffusion
e	extracellular
el	electrical
i	intracellular; i^{th} compartment
j	j^{th} compartment
k	k^{th} compartment
m	membrane
met	metabolic

Subscript	Definition
n	ion species n
o	standard state; initial condition; external compartment
t	tissue; time
T	total

I. INTRODUCTION

In general, it is well established that changes in vascular caliber are normally associated with prior changes in the membrane potential of vascular smooth muscle cells (i.e., depolarization is associated with a decreased caliber and hyperpolarization with an increased caliber) though the detailed mechanisms involved in the contractile processes are not yet known. The transmembrane potential of vascular smooth muscle cells is in turn maintained by an active transport mechanism which pumps sodium ions out of and potassium ions into the cells (52).

This active transport of ions across the cell membranes is balanced in the steady state by diffusive transport in the opposite direction under the influence of electrical and chemical driving forces. Any change in the environment of the cells (such as changes in blood composition) can lead to changes in the active and passive fluxes of ions across the cell membrane, resulting in altered transmembrane potentials of the cells and subsequent contraction or dilation of the vessel.

Particularly, the local effect of altering plasma potassium concentration ($[K^+]$) on the vascular resistance has been intensively studied with intact tissues by many investigators (1, 15, 49). As a result of these studies an electrogenic Na-K pump hypothesis has been suggested (15).

1

The exchange of sodium and potassium ions between muscle cells and surrounding media has also been studied with isolated vascular smooth muscle, in an effort to understand the role of these ions in muscle action at a cellular level. However, none of the past works account for the presence of active pumping of sodium and potassium ions in the analysis of their data. Furthermore, most of the experimental data have been interpreted based on the assumption that the ions are distributed in two compartments, the intra- and extracellular phases, and the only resistance to mass transfer between compartments is localized at the interface between them. If the diffusion process in the continuous extracellular space affects the overall rate of ion transfer in the tissue, this has to be taken into account. With the use of radioactive tracer techniques, it has been shown (25, 35) that there are marked discrepancies between the measured rate of exchange of ions (between tissue and the surrounding medium) and the rate at which the exchange would occur, if the cells had free access to the surrounding medium. This difference was attributed to diffusion in the extracellular space.

In this research, the transport of sodium ions in arteries was studied both theoretically and experimentally, with the use of radioactive tracers. Experimental data on sodium-22 efflux from vascular tissue were analyzed based on a mathematical model which takes into account diffusion in the extracellular space and transport across cell membranes by passive and active mechanisms. The specific aim of this work was to measure the membrane permeabilities

of vascular smooth muscle cells to sodium ions and the active
pumping rates of sodium ions when temperature and potassium ion
concentration in the solutions used for incubating and washing the
tissue were varied. These results are discussed based on the
electrogenic Na-K pump hypothesis.

II. BACKGROUND

Physiological Considerations

Local regulation of blood flow in individual organs in
accordance with the organ's need is a very important body function.
The vascular smooth muscle cells located in the small blood vessel
walls contract or relax in response to changes in the environment
of the cells, changing the resistance to blood flow through the
vascular bed.

The detailed mechanisms involved in this process are not
yet understood. However, with the use of tracer and microelectrode
techniques it has been shown that the contractile process of
vascular smooth muscle is, in general, linked to changes in the
cell membrane potential, which is maintained by active pumping of
sodium ions out of and potassium ions into the cell. Furthermore,
Na^+-K^+ activated ATPase (adenosine triphosphatase) in the smooth
muscle cell membrane is known to be responsible for this active
pumping mechanism.

Structure of the Vascular Wall

The walls of all blood vessels except the capillaries are
composed of four important types of tissues: the endothelial lin-
ing, elastin fibers, collagen fibers and smooth muscle. In all
but the smallest arteries the tissues are arranged in three coats
(see Figure 1).

4

1. Inner coat
2. Middle coat
3. Outer coat
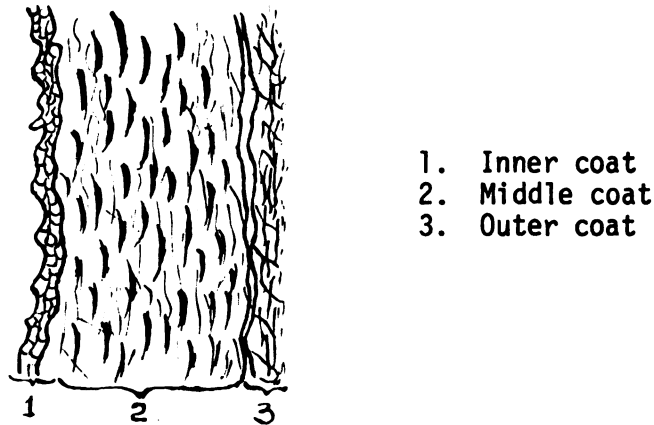
Figure 1.--Transverse section of wall of blood vessel.

The innermost coat consists of a lining endothelial layer, a thin subendothelial layer of fine collagen fibers and a layer of elastic fibers. The middle coat (the media) which is usually the thickest layer of tissue consists of smooth muscle bound together in a spiral shape by elastin and collagen fibers. Composition of blood vessels differs depending on function. In large arteries the predominant tissue of the media is elastic fibers. As the vessels branch and become smaller and more numerous, there is a gradual replacement of elastic fibers in the media by smooth muscle. In the arteries of medium size, the middle coat consists mainly of smooth muscle in fine bundles arranged in lamellae and oriented circularly around the vessel. These lamellae vary in number according to the size of the vessel; the smallest arteries having only a single layer, and those slightly larger three or four layers. The outer coat of the vascular wall consists almost entirely of a

fine and closely matted bundle of collagen fibers but also contains elastic fibers in all but the smallest arteries.

The role of the lining endothelial cells in the circulation is primarily to provide a smooth wall and to offer a selective permeability to substances diffusing from the blood stream to the tissues. The function of elastic fibers is to produce an elastic tension automatically to resist the distending force of the blood pressure. The collagen fibers form networks throughout the media and outer coat and provide a high degree of resistance to distension. The function of the vascular smooth muscle is to produce active tension by contraction under physiological control and thus change the diameter of the lumen of the vessel and regulate blood flow (13).

The Vascular Smooth Muscle Cell

The vascular smooth muscle cells are usually confined to the media and are arranged in a spiral or helical fashion. They are the only cellular elements in the walls of blood vessels other than the single layer of endothelial cells lining the lumen. The smooth muscle cells are long and narrow, and are mainly oriented in a helical fashion around the blood vessel so that lengthwise contraction will cause a decrease in the diameter of the vessel. The cells are more or less fusiform, varying from 30 to 100 μ in length and from 1.5 to 5 μ in diameter in the nuclear region with a sausage-like nucleus (12).

The greater part of a vascular smooth muscle cell consists of a water solution, which is in osmotic equilibrium with the surrounding extracellular fluid. But the solutes are found to be unevenly distributed between the cell interior and the extracellular fluid as shown in Table 1. The concentrations of sodium and chloride are much higher in the extracellular fluid, whereas for potassium the situation is just reversed. There is also a large difference in electric potential across the cell membrane with the inside of the cell being negatively charged with respect to the outside (during inactivity).

TABLE 1.--Representative ion compositions of mammalian smooth muscle (9).

Substance	Concentrations (mEq/1)		Nernst Equil. Potential (mV)
	Intracellular	Extracellular	
K^+	145	4	-96
Na^+	10*	150	+72
Cl^-	17	110	-50
HCO_3^-	8	27	-32
H^+ (pH)	1.25×10^{-4}(6.9)	4×10^{-5}(7.4)	-31
Mg^{++}	1*	2	+19
Ca^{++}	10^{-4}*	5	+289
Glucose	--	5	--
Charged proteins (anions)	140	3	--
TOTAL (mOsm/kg)	300	300	Em = -50

*approximate free ionic concentration.

It is generally accepted that many important differences
exist between vascular smooth muscle and other types of muscle
(cardiac, skeletal). The total amount of sodium and chloride (in
mEq/kg of tissue) are higher and potassium is lower in comparison
with skeletal and heart muscle (21, 56). There are also numerous
reports that vascular smooth muscle cells contain relatively high
intracellular sodium ion concentration (52). The resting membrane
potential of the vascular smooth muscle cell (-30 to -60 mV) is
low relative to that of the skeletal or heart muscle (approximately
-90 mV). The differences in ion concentrations and cell potential
are two striking characteristics of vascular smooth muscle cells.

The Membrane Concept

Although it is a well known fact that cells are bounded
by thin membranes (approximately 75 Å thick), the very definition
of the term "cell membrane" is a matter of contention. In the ana-
tomical sense, the "cell membrane" is the outermost region of the
cell which can be observed as a darkly staining region in the light
microscope. In the physiological sense, the "cell membrane" is a
hypothetical structure devised to explain certain cellular properties
affecting the distribution of substances between the cell and the
extracellular fluid and their rates of transfer into and out of the
cell.

The high intracellular potassium concentration and the
closeness of its equilibrium potential to the cell membrane poten-
tial indicates that the cell membrane must be highly permeable to

potassium ions. The situation with sodium ions is quite different, however. Here the intracellular concentration is considerably lower than in the extracellular fluid, even though the negative potential inside and the higher concentration outside tend to attract sodium in from the extracellular fluid.

For some time it was generally assumed that the cell membrane was specifically permeable to potassium and not to sodium, but the advent of radioactive tracer techniques by 1940 proved that sodium could penetrate the membrane (28). Since then it has been abundantly demonstrated by electrophysiological studies and by tracer studies that the cell membrane is permeable to most, if not all, ions (25, 35).

There are many other observations which have served to strengthen the membrane concept as a "permeability barrier" between the cell and its environment. Among these are the electrical measurements of the cable constants of the muscle fibers, which demonstrate that the cell interior behaves as a good electrolytic conductor which is separated from the external electrolyte solution by an insulating surface layer (20, 30).

The conductivity of this layer appears to be extremely low compared with that of the aqueous phase on either side. Values of 1 to 10^{-4} $ohm^{-1}cm^{-2}$ have usually been obtained. For a membrane 50 $\overset{\circ}{A}$ thick this amounts to a specific resistance of the order of 10^{10} ohm cm, 100 million times greater than that of the surrounding solutions. This is a measure of the low permeability of the cell

membrane to ions, even to the small ions--potassium, sodium and chloride--which are present on either side.

Although the ionic permeability of this surface structure is very low, it shows a remarkable discrimination between the different ion species. Of the major ions encountered in vivo, membranes are especially permeable to K^+ and Cl^- and less so to Na^+. This is of great physiological importance because the cell membrane's relative permeabilities to the principal ions helps to maintain the membrane potential.

In order to explain why the surface membrane behaves as an ionic barrier, that is, a relative insulator between two well-conducting aqueous media, one may assume that the bulk of the cellular membrane consists mostly of a separate lipid phase, possibly no more than a bimolecular leaflet, interposed between the intracellular cytoplasmic gel and the outside solution.

Inasmuch as the cell interior is a different phase from the external medium in which the cell is immersed, it is possible to talk of the surface tension at the cell surface. From the results of interfacial tension measurement on cells, Davson and Danielli (18) deduced their bimolecular leaflet model for the structure of biological membranes. According to this model, the basic construction of all biological membranes consists of a bimolecular lipid leaflet (bilayer) with adsorbed nonlipid layers (mostly proteins). The lipid molecules are oriented with their polar groups facing outward and their hydrocarbon chains away from interfaces forming the interior of the membrane.

Since then, this hypothesis has been the basis of almost all work in the exploration of membrane structure and function. The most recent technical advances of electron microscopy and X-ray crystallographic analysis have confirmed the major part of this model.

One of the most generally valid findings of current electron microscopy (47) is the demonstration of the presence, at the limiting surface of almost all cell types studied, of a layer of material some 75 $\overset{o}{A}$ thick which is a composite, being made up of two dark layers each about 25 $\overset{o}{A}$ thick and separated by a light layer of some 25 $\overset{o}{A}$. Under the electron microscope, vascular smooth muscle cells have also been found to have a distinct cell membrane, which is about 70 to 100 $\overset{o}{A}$ thick and is in fact composite. As in most other types of cells, it is also made up of two dark layers separated by a light layer (12).

The functional boundary between the intracellular and extracellular fluids is now generally believed to be a thin (75 $\overset{o}{A}$), highly organized, bimolecular lipoprotein layer which severely restricts the interchange of substances. Membranes are, therefore, basic elements of all biological structure, enabling the cells to maintain the internal composition at a quite constant level through the regulation of the passage of substances into and out of the cell and also supplying a matrix for the orderly organization of cell constituents. Continued existence of the cell is entirely dependent on these characteristic properties of the membrane.

The Membrane Potential

A membrane potential is simply an electrical potential dif-
ference which exists across a cell membrane because of a separation
of electrical charges. The charge may be either ionized protein
molecules, perhaps attached to the cell membrane, or simple ions
such as Na^+, K^+, or Cl^-. In general, membrane potentials can be
considered to be either resting potential or action potential,
depending upon their rate of change. A membrane potential is a
resting potential if it is changing either slowly or not at all.
The resulting membrane potential of the vascular smooth muscle cell
is reported to be about -30 to -60 mV (52), which is low compared
to those of other types of muscles. On the other hand, when an
action potential occurs, membrane potential rapidly increases from
its resting value, often to a positive value, and returns to its
resting value within a very short time (order of one millisecond)
as shown in Figure 2.
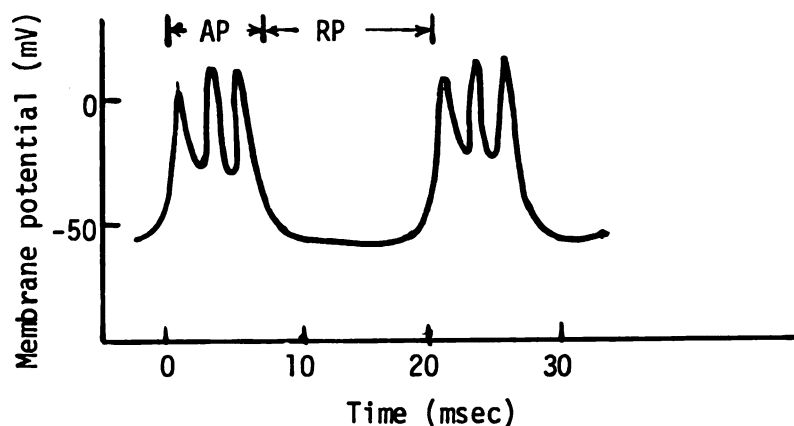
Figure 2.--Schematic representation of membrane potentials
across the cell membrane. AP = action potentials, RP = resting
potential.

The membrane's relative permeabilities to the principal ions and the relatively high resistance to ionic flow through the membrane are responsible for the membrane potential and the potential is maintained by an active transport mechanism which balances out the net passive fluxes of ions under steady state.

Electric potential differences, in general, appear at the boundaries between two electrolyte solutions if there are ions of different mobility or concentration on either side. In the absence of a membrane, one obtains a "liquid-junction" potential or diffusion potential. Suppose two dilute aqueous solutions of NaCl at different concentrations are making contact through a porous media. A diffusion potential will immediately develop because Cl^- ions in aqueous solution are more mobile than Na^+ ions. The potential difference across the barrier can be calculated from the formula (22)

$$E = \left(\frac{RT}{F}\right) \left(\frac{u - v}{u + v}\right) \ln \frac{C_1}{C_2} \qquad (1)$$

where R is the universal gas constant; T the absolute temperature; F the Faraday (electric charge per gram equivalent of univalent ions); u and v the mobilities of Na^+ and Cl^-, respectively, along the potential gradient; and C_1 and C_2 the salt concentrations (or more correctly, the geometric mean activities of the two ions) on each side.

If a semipermeable porous membrane is placed across the boundary, the resulting potential difference will depend on the

nature of the membrane used and on the concentrations of the ions on its two sides. If the membrane pores are so large that all molecules and ions of moderate size can penetrate, only large colloidal particles like protein being excluded, diffusion takes place and a liquid junction potential will appear. The magnitude of this potential depends on the differential ionic mobilities within the membrane pores and on the concentrations on either side. The system is not in a steady state, but gradually runs down unless the concentration gradients are continuously restored by an active pumping process.

At electrochemical equilibrium across a membrane the sum of electrical plus chemical potentials of each ion on either side of the membrane become equal:

$$z_n FE_1 + \mu_{n,1} = z_n FE_2 + \mu_{n,2} \tag{2}$$

also

$$\mu_n = \mu_{0,n} + RT \ln a_n \tag{3}$$

where E_1 and E_2 are the electrical potentials on both sides, respectively; z_n the valance of ion n; μ_n the chemical potential of ion n; $\mu_{0,n}$ the standard state chemical potential of ion n, and a_n the chemical activity of ion n. Substituting the expression for the chemical potential into Equation (2) and rearranging,

$$E_1 - E_2 = E_m = \frac{RT}{z_n F} \ln \frac{a_{n,2}}{a_{n,1}} \tag{4}$$

Equation (4) is the well known Nernst equation and gives the electrical potential difference across the membrane at equilibrium. If it is assumed that the activity coefficient for ion n is the same on each side of the membrane, then the activity terms can be replaced by the concentrations:

$$E_m = \frac{RT}{z_n F} \ln \frac{C_{n,2}}{C_{n,1}} \tag{5}$$

The Nernst equation is one of the best known and frequently cited equations in the biological literature. Many different theories of bioelectric phenomena are based on some variant of this extremely useful formula.

Actually, biological cells are normally in a steady state maintained by some active transport mechanism rather than in a true thermodynamic equilibrium state. This must be so since otherwise the gradients would soon disappear (i.e., the cell would "run down"). The exact mechanism by which individual ions are actively transported is not known. However, it is generally believed that a "sodium-potassium pump" constantly extrudes sodium and takes up potassium. The pump is supposedly located in the cell membrane and uses metabolic energy provided by the breakdown of adenosine triphosphate (ATP) to adenosine diphosphate (ADP). Furthermore, the rate of transport of sodium is usually greater than that of potassium. Thus, the pump is

not electroneutral, but in fact transports net positive charge
out of the cell. This characteristic is referred to as electro-
genic and Thomas (55) points out that the experimental evidence
indicates that few, if any, tissues exist for which the Na-K
pump is electroneutral.

Since metabolic energy is consumed by the electrogenic pump,
the direct contribution of the pump to the total resting potential
is referred to as the metabolic potential. The diffusion potential
(E_{dif}) due to the passive ionic fluxes and metabolic potential
(E_{met}) sum to produce the resting membrane potential:

$$E_m = E_{dif} + E_{met} \qquad (6)$$

Because of the interest of physiologists in the ionic
permeability of the cell membranes and in cell potentials, both
of these properties have been studied extensively. In connection
with these studies a number of models for the biological membrane
have been proposed in an attempt to gain insight into the events
within the membranes. Among them are the Plank membrane, the fixed
charged membrane, and constant field membrane (Goldman model) (15).

Electrophysiological studies of membrane phenomena attempt
to correlate transmembrane potentials, ionic compositions, and
ionic fluxes based on the membrane models, deriving theoretical
interconnections as an aid in the interpretation of experimental
data. The relationship between ion fluxes and transmembrane

potential is complicated and depends on the specific membrane model used. If the transmembrane potential is changing so slowly that capacitative current is negligible, Goldman's constant field model yields an accurate relationship given as follows,

$$E_m = \frac{RT}{F} \ln \frac{rP_K[K^+]_e + P_{Na}[Na^+]_e + P_{Cl}[Cl^-]_i}{rP_K[K^+]_i + P_{Na}[Na^+]_i + P_{Cl}[Cl^-]_e} \qquad (7)$$

where r is the exchange ratio of the Na-K pump (defined as the ratio of the pumping rate of Na^+ to that of K^+), and P_K, P_{Na}, and P_{Cl} are the membrane permeabilities to potassium, sodium, and chloride ions, respectively.

Though a great deal of work has been done in the past toward measurement of cell potentials and of ion permeabilities in various bathing media, there are very few examples of vascular smooth muscle cells for which both types of experimental data are available.

Ion Transfer Through the Cell Membrane

Transport of a substance across a cellular membrane is called passive if the process can be accounted for by means of ordinary physical forces: those caused by a concentration gradient, an electrical potential gradient, a solvent drag, or any combination of these. Active transport processes, then, are those which cannot be explained as the result of these forces, but involve participation of some energy-yielding chemical reaction. Active transport processes have commonly been classified as those where

the substance in question is moved against an electrochemical gradient; in other words, the substance gains free energy by the transferring process. This extra free energy is delivered by the metabolism of the cell. The nature of active transport has still not been fully explained, but it is generally believed that chemical reactions with membrane constituents are necessarily involved.

Passive Transport

It has become common usage to call passive transfer of an ion "diffusion" if brought about by differences in either chemical or electrical potential or caused by solvent drag. The ions in dilute aqueous solution exist in hydrated form. These hydrated ions are several times larger in diameter than the corresponding naked ones and are so far apart that they may be considered to move independently of each other. Such independent movement is often referred to as free diffusion in contradistinction to diffusion restricted by small pores or by interaction between diffusing particles. A porous membrane having pores large on a molecular scale would, if placed in a concentration gradient, reduce the cross section available for diffusion and possibly increase the distance, but diffusion would otherwise be unaffected. Such large pores also would permit bulk flow of the solution as a whole when there is a gradient of hydrostatic pressure to provide energy. This flow of the liquid in bulk would profoundly modify exchange by diffusion, for fluxes in the direction of the stream will be

augmented and the opposite fluxes diminished or even reversed, causing a solvent drag effect, as in the walls of capillaries. It has not been shown that this occurs in the cellular membranes.

With small pores, not much larger than the solute molecules, the effect of bulk flow becomes less important. However, a new complication appears in that steric factors and in the case of ions, surface charges on the material of the pores begin to interfere with free diffusion. Moreover, when solutes of several molecular sizes are present, the restrictions upon diffusion become selective, and the tendency for different molecular species to be separated is far greater than when diffusion takes place in free solution. Exchanges through pores of this size involve both bulk flow (when there is a gradient of hydrostatic pressure) and restricted diffusion. The relative contributions of each depends upon the sizes of the pores and the permeating molecules. It is often convenient to focus attention upon the relative ease with which different substances cross a membrane by speaking of them as being more or less permeable to them and by describing the rate of exchange of each substance by a permeability coefficient rather than by a modified diffusion coefficient. Since the path length through the membrane is usually indeterminate, the rate of transfer is often expressed in terms of the difference in concentration between two sides, and the unknown path length is incorporated into the permeability constant.

Pores smaller than the solvent and the smallest solute molecules would not permit exchange by either bulk flow or diffusion,

but penetration through pores may not be the only way across a membrane. Homogeneous (nonporous) membranes may be crossed by molecules which can dissolve in or combine with their substance, diffuse across in solution, and then re-enter the liquid phase at the other side. The concentration ratios between the bulk phase and the membrane at each boundary depend upon the partition coefficient between the membrane substance and the liquid at either side. These partition coefficients, together with the activation energy which may be necessary for a molecule to shed its hydration shell and pass from the aqueous phase into the membrane help to determine the concentration gradient within the membrane, and consequently the rate of diffusion across it. Such membranes allow permeation by a form of restricted diffusion with no provision whatever for bulk flow under gradients of hydrostatic pressure.

There has been much argument whether solutes cross biological membranes through pores or by dissolving in the membrane. Opposite opinions in the controversies have often been partly correct. Membranes may exhibit pores in a surrounding building material which can itself be an additional channel for diffusion of substances which are soluble in it.

Active Transport (The Na^+-K^+ Pump)

One of the great mysteries of nearly all living cells was how they maintained a relatively high potassium and low sodium content, while they were surrounded by interstitial fluid with a reversed concentration ratio of the two cations and the membranes were permeable to the ions.

The results of many studies related to this question led to the so-called "pump-leak" concept: the cell membrane allows a passive leakage of both ions down their electrochemical gradients, while an active pump system extrudes sodium ions and draws potassium ions into the cell against these gradients. Under steady state these passive fluxes are balanced by the active fluxes.

Since work must be done to carry sodium ions from a region of lower to a region of higher electrochemical potential, it is obvious that energy derived from cellular metabolism must be used for the active transport. Early studies (29, 42) have shown that the ATP produced by cellular metabolism is an energy source sufficient to maintain pumping. More direct evidence for this comes from experiments in which ATP was placed inside cells lacking any other energy source. Microinjection of ATP into a squid giant axon poisoned with metabolic inhibitor restored the sodium efflux (36).

In an effort to identify the pump system, Skou (5) reasoned that an enzyme, ATPase, would be required to make the energy of ATP available to cation transport and that this enzyme might require Na^+ and K^+ for activity. This enzyme hydrolyzes ATP to ADP and in the process releases energy. In a study of a crab nerve fiber he was able to demonstrate a Mg^{++} activated ATPase activity, which was increased considerably upon addition of Na^+ and K^+ to the assay medium and that this additional ATPase activity was completely inhibited by ouabain. Its properties closely resemble those of the Na^+-K^+ pump. Therefore, Skou suggested that this ouabain sensitive,

Na^+-K^+ activated ATPase (Na-K ATPase) might be part of or identical with the cation transport system.

Since the work of Skou, a great number of reports have been published confirming this conclusion for a variety of cells and tissues and it has now become well established that the enzyme system known as Na-K ATPase is involved in the transport of cations across many types of cell membranes (51, 55).

Ion flux studies on vascular smooth muscle indicate the existence of an active sodium pump (17, 21, 24, 34). Sodium efflux from pieces of rabbit aorta (17), for example, is inhibited by ouabain and other metabolic inhibitors, K-free solutions, and cold. One characteristic of sodium efflux in arterial muscle is its high potassium dependency. About 90% (of normal sodium efflux) reduction by potassium-free media is observed in dog carotid arteries as compared to 40-50% in striated muscle and 30% in red cells (21). Ouabain and potassium-free solutions have also been found to increase tissue sodium and to decrease tissue potassium (17, 21). It appears that these changes in ion content of the arteries after addition of ouabain are due to changes in the cellular pool. This effect can be interpreted as due mainly to a reduction of the active pumping of sodium out of and potassium into the cells.

The evidence thus indicates that active cation transport in vascular smooth muscle occurs by a mechanism similar to that in other tissues and hence that a Na-K ATPase exists in this tissue.

Bonting and co-workers (6) were the first to report Na-K ATPase activities in homoegenats of various smooth muscle tissues

including that of rabbit aorta. The activity was stimulated by
the addition of Na^+ plus K^+, although this stimulation was only
slight. Recently, a Na^+ and K^+ stimulated, Mg^{++}-requiring ATPase has
been successfully demonstrated in the membrane preparations of
rabbit vascular smooth muscle by Wolowyk et al. (58). It is shown
that the rate at which sodium and potassium ions are actively trans-
ported is dependent upon the extracellular potassium concentration
($[K^+]_e$) and intracellular sodium concentration ($[Na^+]_i$). Since
the active transport is coupled, a decrease in $[K^+]_e$ will not only
reduce K^+ uptake, but also Na^+ extrusion by the pump. Conversely,
increases in the concentrations of these ions stimulate the
activity of the pump.

Contraction of Vascular Smooth Muscle

Structural Basis of Contraction

In contrast to striated muscles, smooth muscles are a
heterogeneous group that show great diversity both in their morpho-
logic arrangement and in their physiologic properties. Because of
these diverse morphologic and physiologic properties, it is diffi-
cult to make generalizations about the fundamental properties of
smooth muscles.

The cytoplasm of vascular smooth muscle cells is packed
with contractile myofilaments, which may not be arranged in dis-
tinct sarcomeres as in striated muscles, and run approximately
parallel to the long axes of the muscle cell. A large portion of
vascular filaments are typical thin, actin filaments, but there is

some debate about the presence of thick myosin filaments. However, a protein with chemical properties similar to myosin has been isolated from various types of smooth muscle cells (52). It may be that the failure so far to demonstrate more than a few, if any, myosin filaments in intact smooth muscle might not be because of their absence, but rather because of the problem of finding a technique capable of demonstrating them under the unusual conditions of myosin activity characteristic of this tissue. On the other hand, it may be that myosin is present as dissolved monomers, being induced to aggregate to form filaments under certain conditions. Even though in the case of smooth muscle the picture is still not as clear as one could wish, it is generally believed that smooth muscles contain both actin and myosin (52). Furthermore, the sliding-filament model of muscle contraction which depends on the existence of the two types of myofilament within a muscle fiber is suggested to be applicable to smooth muscles (43).

Electron microscopic studies of the vascular wall show that smooth muscle cells do not constitute a true anatomic syncytium, in that a distinct plasma membrane surrounds each cell with no direct cytoplasmic continuity between adjacent cells (12). The individual cells are arranged in branching bundles, surrounded by connective tissue sheaths and these bundles rather than individual muscle cells are believed to be the effector units in smooth muscle systems (12). Therefore, the exact relationship of the muscle cells to each other within a bundle is of great functional significance.

Many workers have reported the presence of areas of close contact between muscle cells in different tissues (12). It is now well established that there are areas of close contact between smooth muscle cells within effector bundles, taking the form of "bridges" or "intrusions" depending on the types of cells. About 3-5% of the total surface area of a muscle cell has specialized regions of contact with neighboring cells (12).

Intercellular connections provide a means of direct transfer of information from one cell to another. For instance, electrical transmission may be impossible over large intercellular distances because of short circuiting of extracellular fluid. It has been suggested that in smooth muscle specialized areas of close contact provide the low resistance pathway for conducted electrical activity (52).

Smooth muscles may be classified into two groups according to their physiologic properties: unitary muscles and multi-unit muscles (7). The unitary muscles are characterized by spontaneous activity initiated in pacemaker areas within the tissue which spreads throughout the whole muscle as if the muscle were a single unit. Multi-unit muscles do not contract spontaneously and normally are activated in more than one region by multiple motor nerves. Another property of unitary muscle is its ability to respond to stretch by developing active tension while multi-unit muscle does not react to stretch by developing tension.

Vascular smooth muscles do not fall clearly into one or the other of these two groups but combine properties from each category.

The large arteries are not spontaneously active and they do not
respond to stretch by developing active tension. They contain many
nerve fibers within their walls and presumably are normally activa-
ted, mostly by nerve stimulation. The behavior of small terminal
arteriols and precapillary sphincters and some veins resembles that
of unitary muscles in many respects. These vessels show a con-
siderable amount of spontaneous motility that is accompanied by
slow oscillations of the membrane potential and action potentials.
Their spontaneous activity is increased by stretch.

Activation of Muscle Contraction

The basic physiologic function of a muscle is to develop
tension, which is then linked to a variety of body functions.

The ionic and electrical characteristics of a muscle are
highly relevant to an understanding of how activation of the con-
tractile mechanism is initiated.

Role of the calcium ion.--The calcium ion is essential for
the contraction of smooth muscle. It participates in one link of
the chain of events leading to a normal contraction; it triggers
the release of mechanical energy by inactivating a relaxing factor
(troponin) bound to the contractile protein (which is myosin).

There is considerable evidence that in smooth muscle a rise
in free intracellular Ca^{++} activates contraction and a fall in
cytoplasmic Ca^{++} activity leads to relaxation (52). This source of
activator Ca^{++} may arise from an increased influx of the extra-
cellular ion or from translocation of Ca^{++} bound at the surface

membrane or concentrated in an intracellular storage site. The exact source of the Ca^{++} and the mechanism of its release still remain to be established. Electron microscopic studies have shown that the endoplasmic reticulum is poorly developed in smooth muscle, indicating the importance of the extracellular Ca^{++} (12). Several isotope studies have demonstrated that Ca^{++} influx increases during contraction of smooth muscle (10, 46). Many more studies have presumed that an increase in Ca^{++} influx occurred because a greater response was observed when extracellular Ca^{++} concentration was increased over a given range (0.6 to 2.7 mM/l) (41). From this evidence it appears that the calcium ions, in the case of vascular smooth muscle, probably enter from outside the cell and are not, as in skeletal muscle, released from particulate stores of Ca on the inner surface of cellular membrane. The permeability of the membrane to Ca^{++} thus is of paramount importance in vascular smooth muscle.

Because of the direct dependence of the contractile process of smooth muscle on the Ca^{++} ion, it is common practice to attribute the action of the other electrolytes and of physiological and pharmacological agents to their effect on the calcium ion.

Electrical-mechanical coupling.--It is now generally accepted that in mammalian fast striated muscle fibers the initiation of contraction is mediated by the action potential which triggers the release of Ca from the sarcoplasmic reticulum, raising free myoplasmic Ca^{++} to the critical level required for activation of the actomyosin system through the inactivation of troponin bound

to the contractile protein. Since the troponin prevents the chemo-mechanical transduction by the ATP-actomyosin system this inhibitor action of Ca^{++} causes the initiation of contraction by allowing a sliding motion of this actin fiber over a thick myosin fiber (5). In contrast, the detailed mechanism of electromechanical coupling in smooth muscle has not been fully elucidated.

It appears that there exist two major electrophysiologic types of vascular smooth muscle, one gradedly responsive and the other producing repetitive action potentials.

Action potentials in spontaneously contracting vascular smooth muscle, and their association with contraction, have been shown to occur in various types of vascular smooth muscles (53). The degree of contraction seems to be determined by two mechanisms: (1) regulation of the number of active, firing fibers; (2) variations in action potential frequency.

Graded depolarization, rather than action potentials, appears to be the normal electrical response of certain types of vascular smooth muscle. This mechanism seems to be operating on those types of vascular smooth muscle which display no spontaneous electrical activity or contraction (52, 53). The coupling mechanism that links the graded depolarization of vascular smooth muscle in large multi-unit vessels to contraction is also uncertain. One possible mechanism may be that depolarization in this type of smooth muscle produces a maintained increase in Ca^{++} permeability.

Based on observations of a close connection between electrical and mechanical activities, it may be said that in vascular

smooth muscle, a change in membrane potential, be it by transient or sustained depolarization, initiates contraction.

However, the role of electrical process in the electrical-mechanical coupling of vascular smooth muscle has been the subject of conflicting reports. Many examples can be cited in which (1) action potential occurs without a mechanical response (uncoupling) or (2) tension is developed or maintained in the absence of changes in membrane potential.

Pharmacomechanical coupling.--Although depolarization, whether transient or sustained, normally leads to or is associated with the activation of the contractile mechanism, there is evidence that drugs can affect excitation-contraction coupling by a mechanism that is not entirely dependent on depolarization of the membrane. Waugh (57) demonstrated that contraction could occur in vascular smooth muscle in response to epinephrine in the absence of changes in membrane potential. In the pulmonary artery, Su et al. (54) obtained tension responses to drugs without change in potential. Tension responses to drugs which could apparently not be accounted for by changes in electrical activity have been reported and discussed in detail by Somlyo and Somlyo (53). They also named this form of excitation-contraction coupling, independent of potential changes, as pharmacomechanial coupling. It has been suggested that the ability of drugs to translocate Ca into the cytoplasm from a compartment not accessible to depolarization is responsible for this initiation of contraction (53). However, these are rather special

experimental studies, that may have no relation to real life. The detailed mechanism of pharmacomechanical coupling remains to be determined.

Role of the potassium ion.--There has been a great deal of research to relate the intracellular concentration or the trans-membrane gradients of monovalent ions directly to the contractile process in vascular smooth muscles. Particularly, the effects of changes in plasma $[K^+]$ on the resistance to blood flow in various vascular beds have been intensively studied (1, 15, 49).

A decrease in the plasma $[K^+]$ of the blood perfusing the gracilis muscle of the dog produces vasoconstriction (1), whereas increased plasma $[K^+]$ does the reverse (1, 15).

As pointed out above, changes in vascular resistance are generally associated with changes in membrane potential of the vascular smooth muscle cells, i.e., depolarization is associated with vasoconstriction and hyperpolarization with vasodilation.

The depolarization (9) and contracture induced by decreasing plasma $[K^+]$ are probably a direct effect, and not due to release of some vasoactive agents. This depolarization of vascular smooth muscle may be brought about either by changing the passive perme-ability of the membrane to some ionic species or by changing the activity of the electrogenic Na-K pump, or both.

With the assumption of constant permeability, Brace (9) tested the electrogenic Na-K pump hypothesis by a mathematical study of the smooth muscle cell, concluding that an electrogenic

Na-K pump was essential to the vascular contraction induced by changing plasma $[K^+]$. Of course, the effect of changing pump activity on the membrane potential will depend on the coupling ratio of the pump, which might be variable.

For a better understanding of the mechanism involved in the depolarization of vascular smooth muscle induced by lowering plasma $[K^+]$, the effect of changing $[K^+]$ on the permeability of vascular smooth muscle must be investigated as well as the effect on the pumping rate.

Some other mechanisms, i.e., interference with a K-dependent Ca pump or Ca permeability, may also contribute to the contraction induced by lowering plasma $[K^+]$, particularly for the case of K-free contracture (52).

III. KINETICS OF ION TRANSFER

It is well known that ionic compositions and their gradients influence the electrical polarization of cells and therefore their excitability. A knowledge of the ionic compositions and the processes controlling ion transport in vascular walls is essential to the understanding of not only the electrical properties but also of the basic physiological functions. In an effort to characterize the basic properties of ion transport mechanisms, many kinetic mass transfer studies have been done on vascular smooth muscles (17, 21, 24, 33, 34, 39, 40). The studies have not, however, led to a uniform interpretation of the underlying mechanisms.

One area of development was the application of the membrane concept to the ion transport phenomena. The cell membrane was taken to function as a discrete resistance for the exchange of material between two well mixed intra- and extracellular fluids. As pointed out earlier, various mechanisms have been postulated for the movement of ions across the smooth muscle membrane including diffusion of independent ions, diffusion of ion pairs, coupled sodium-potassium exchange via an active transport mechanism, and sodium-sodium exchange via carrier diffusion.

The adoption of membrane models to smooth muscle behavior has not been universal. In some studies, bulk properties of the smooth muscle cytoplasm rather than membrane properties were

emphasized in the interpretation of ion transport mechanisms (7, 33). Based on ion-protein-water interactions in the cell cytoplasm, a theory of cellular behavior called the "association-induction hypothesis" was formulated by Ling (37). According to this theory, electrolyte contained within the cell is in two states, either dissolved in the interstitial water or adsorbed onto fixed sites. The membrane and cytoplasmic phases are considered as part of the same continuum.

However, current accumulation of evidence favors the membrane model for interpreting kinetic transport data for muscle tissues. It is, therefore, usually assumed that ions are distributed between the intra- and extracellular spaces, separated by thin membranes, though this is an oversimplification for the vascular wall because of its complex structure.

The kinetic studies with vascular tissue have been mainly concerned with the exchange of sodium and potassium ions between the tissue and surrounding fluid. Most of the studies on sodium transfer rates in vascular smooth muscle indicate the existence of an active sodium pump (17, 21, 24, 34). Generally, the sodium efflux is found to be reduced by low $[K^+]_e$ and low temperature and also to be sensitive to the presence of ouabain in the bathing medium. Thus, the results are interpreted as a reduction in the active transport process. The experimental data have been mostly analyzed by a graphical method, based on the compartmental theory (discussed in detail later).

Extracellular Space and Bound Ions

The understanding of the ion transport properties of vascular walls calls for the knowledge of ionic content in each space under the experimental conditions chosen. For most biological systems such as vascular smooth muscle, isolated measurements of the fluid in each space are not possible. Therefore, it becomes necessary to use auxiliary chemical substances (e.g., inulin, sucrose) which are assumed to penetrate only the extracellular space if information about space distribution is desired. From knowledge of the total tissue ions and of the extracellular space as determined from the chemical indicators, intracellular ion concentration can be evaluated.

There is some doubt concerning the size of the extracellular space of vascular smooth muscle. The chief difficulty met in the measurement of extracellular space of vascular smooth muscle is its heterogeneous structure. There are great amounts of collagen and elastic fibers and mucopolysaccharides which are believed to prevent a uniform distribution of chemical indicators of large molecular size such as inulin throughout the extracellular space. Thus, different values for extracellular volume are obtained depending upon the chemical indicator used.

Another difficulty associated with the evaluation of the ion distribution in vascular wall is the possible presence of bound ions. There is convincing evidence that some ions in vascular smooth muscle are bound in an osmotically and electrochemically inactive state.

Analysis of the distribution of sodium in dog carotid artery with disrupted cells (26) or under metabolically inhibited conditions (56) indicated that this tissue contained much more Na than could be accounted for as being in equilibrium with its environment. A comparison of inulin distribution and sodium exchange properties of freshly dissected dog carotid also indicated an excess Na (21).

The bound fraction of sodium which is characterized by non-diffusibility, though replaceable with different ion species under favorable conditions, has been assumed by some authors to be entirely extracellular (mainly on mucopolysaccharides) whereas others have suggested that some of it is intracellular (5, 26, 33).

Poor definition of the extracellular space and difficulties in quantifying the bound, non-diffusible fraction make calculation of free intracellular ionic concentration very uncertain. Although there is fairly good agreement as to the total ionic content of smooth muscle, no agreement has been reached between different workers concerning the exact distribution of ions in extra- and intracellular spaces.

Radioactive Tracer Techniques

With the use of artificial radioactive isotopes and the development of sensitive means for the measurement of radioactivity, tracer techniques have become one of the most powerful techniques for biological investigations, particularly for studying the dynamics of ion transport across cell membranes. Dynamic aspects of ion transport properties of the vascular wall are studied by

measuring radioactive isotopes entering or leaving the tissue as a function of time, under steady-state physiological conditions. This approach yields information concerning the rate of ion transfer across the cell membrane.

The fundamental property that makes it possible to use radioisotopes as tracers is that all the radioactive isotopes of an element have identical chemical properties. The distinctive physical property which serves to detect and measure the concentration of the isotopes in question is assumed not to interfere with the chemical or the physical processes that the element may undergo.

The radiotracer technique consists of incubating a specimen of tissue in a physiological salt solution tagged with radioisotope. This permits subsequent assay of the amount of the tracer which is in the system at any time during the experiment. A curve relating the amount of the ion transferred from solution to the tissue (or vice versa) to the time elapsed can be determined for the tracer. When the external concentrations have been properly selected the total concentration of the ion being studied does not change in the chemical sense. It is the change in the proportion of tagged substance which allows the transfer to be followed. The radioactive tracer method, therefore, affords an almost ideal approach to the measurement of cellular permeability because it makes possible the study of ion transfer under conditions where there is no net transfer of substances being studied.

Compartmental Analysis (Well Mixed Compartments)

Many investigators have analyzed tracer washout studies with a model consisting of one or more well mixed compartments. The compartments are in series as shown in Figure 3.
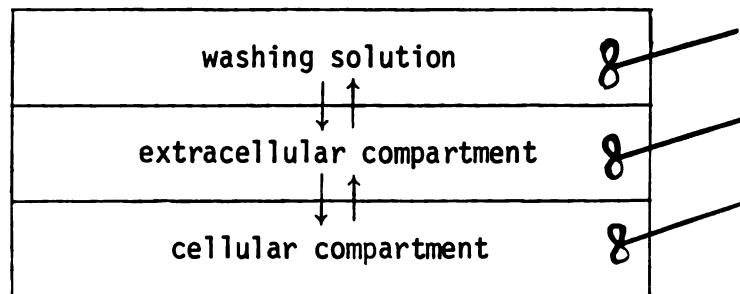
Figure 3.--Two-compartment model of the vascular wall.

It is usually assumed that within a given compartment the substance being studied is uniformly distributed at all times and the resistance to transport between compartments is localized in a single sharp step at the interface between compartments. This assumption implies instantaneous and homogeneous mixing within the compartment and may be a serious weakness of the theory in a practical situation.

Compartmental analysis is concerned primarily with the development of models which reproduce the kinetics of tracer distribution in the biological systems, revealing the presence of barriers to tracer movement in the system. This analysis does not provide information on the physical sizes of the compartments and

tracer distribution. Often, no attempt is made to attach physical significance to the parameters which describe the washout. Active transport is usually ignored. In general, prior knowledge of the size of each compartment and distribution of substance being studied among the compartments is required.

The driving force for the net transport from one physiological compartment to another is usually taken to be the electrochemical potential gradient. In the steady-state condition these forces remain constant. When the tracer is added to a system in the steady state, the driving force for the tracer movement becomes the gradient of the specific activity of the tracer (specific activity is defined as the ratio of tagged to total amount of the compound). The equations governing tracer movement in compartmental analysis, therefore, follow first-order kinetics.

When the processes under consideration can be shown to be first-order, their mathematical description becomes particularly simple and, needless to say, extremely useful. The unidirectional transfer rate of tracer from one compartment to another becomes proportional to the amount of tracer in the former compartment and is described by a linear first-order differential equation.

Considerable work has been done on the analysis and interpretation of kinetic data in terms of linear compartmental systems (3, 4, 48). A linear compartmental system is usually specified by the number of compartments and by transfer rates between compartments. The system can be represented mathematically by a set of first-order differential equations

$$\frac{df_i(t)}{dt} = \sum_{j=1}^{n} \lambda_{ij} f_j(t), \quad i = 1, 2, \ldots, n \tag{8}$$

where $f_i(t)$ represents a function, such as amount of substance, specific activity, etc.; λ_{ij} are the transfer rates per unit time from j^{th} into the ith compartment, and λ_{ii} is defined

$$\lambda_{ii} \geq - \sum_{\substack{k=0 \\ k \neq 1}}^{n} \lambda_{ki} \tag{9}$$

λ_{0i} represents "loss" from the ith compartment to the outside. When the $[\lambda_{ij}]$ matrix has distinct eigen values, the solution of Equation (8), for constant λ_{ij}, are sums of exponentials:

$$f_i(t) = \sum_{j=1}^{n} A_{ij} e^{-\alpha_j t}, \quad i = 1, 2, \ldots, n \tag{10}$$

where the $-\alpha_j$ are the eigenvalues of the $[\lambda_{ij}]$ matrix and A_{ij} are elements of the eigenvectors. In matrix notation

$$[\lambda] = [A] [\alpha] [A]^{-1} \tag{11}$$

Therefore, in compartmental analysis a key point is the fact that the experimental data must be a linear combination of exponentials and that the number of compartments for a model must be chosen to equal the number of exponentials in the fit. However, the basic problem as to how many exponentials are necessary to fit a set of data has not been fully resolved.

The inverse problem of calculating the λ's from experimentally determined values of A's and α's is the usual goal of compartmental analysis. Two approaches have been developed toward this goal. These are discussed below.

Graphical Method

Because of its simplicity and visual effect, graphical methods have been most extensively used for the interpretation of kinetic data based on the compartmental analysis.

To facilitate analysis, the experimental data, consisting of periodic measurement of total amount of the tracer in the tissue as it is washed, are plotted on semilog paper with a linear time axis. By fitting a straight line to the tail end of the curve and extrapolating it to zero time, a single exponential curve is obtained. This straight line is then subtracted from the overall experimental curve and the procedure repeated until the original curve is completely resolved into its exponential components (see Figure 4).

From the analyzed curve the coefficients A_{ij} are obtained by extrapolating each component back to zero time. The parameters α_j are also obtained from the component curves by their relation to half-times, $\alpha_j = 0.693/t_{1/2}$.

As a matter of fact, fitting of experimental data to a sum of exponential does not directly yield much information as to how compartments are interrelated in the physiological domain except in a few special cases. For a biosystem made up of compartments in
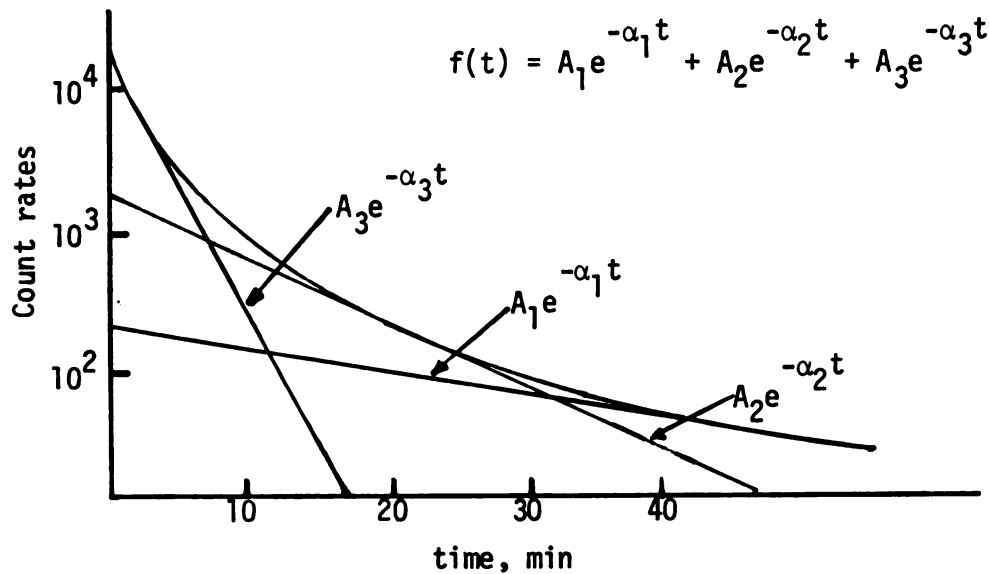
Figure 4.--Analysis of washout data with the graphical
method for a case of the three-compartment system.

series without back diffusion of mass, the overall transfer rate

constants for the individual compartments can be obtained directly

from the exponential factors in the equations describing the

experimental data (48).

But usually the exponential factors α_j have a more compli-

cated interpretation as shown in Equation (11). When the back

diffusion of the substance of interest is involved, each physi-

ological compartment is characterized by a sum of components from

each exponential factor. More exact kinetic models are necessary

for a meaningful representation of exchange of substances rather

than the simple graphical method. Furthermore, it is often dif-

ficult to resolve the experimental curve into exponential

components, unless the parameters α_j differ in magnitude by a factor of two or more.

One of the common pitfalls in using this method is that when postulating kinetic models relating to extracellular and intracellular compartments as in the case of muscle tissues, one is tempted to ascribe the fastest exponential to the dynamics of the extracellular compartment and a slower exponential to that of the intracellular compartment. This assumption would only be true if all the different compartments were open to the outside without recycling between the compartments, but from the structure of the tissue it can be shown that only the extracellular space communicates with the exterior without any specialized energy barrier. There is also a back diffusion of mass between the two compartments. The possible errors of this type of analysis have been shown (31).

Berman's Analytical Method

In general, compartmental analysis requires observational access to all compartments and also their interrelation with regard to the spatial configuration. Berman and Schoenfeld (3) developed a mathematical treatment which was more flexible than previous approaches (48). This method overcame some of the limitations imposed by the usual procedure of having to assume a biological model and of requiring experimental access to all compartments.

In their approach, a definite model does not have to be assumed before the data can be analyzed. A model having a number of compartments equal to the number of exponential terms in the equation

describing the data for the accessible compartments is first pro-
posed. Then, a set of invariants is defined in terms of the
coefficients (A_{ij}) and exponential factors (α_j) found in the curve
fitting. These are related to the transport rates (λ's) as follows:

$$[\lambda] = [A]\ [\alpha]\ [A]^{-1} \tag{11}$$

The degrees of freedom of the model are expressed in terms of a
minimum number of variables equal to the difference between the
number of variables and the number of known invariants. They are
evaluated from the known A's, α's and a generating model given by a
matrix $[\lambda]$ consistent with the known invariants. From a linear
transformation of the matrix $[\lambda]$, other mathematically consistent
models are "mapped" and then the restrictions set by physical possi-
bilities are imposed. Depending on how much information is available,
a set of possible models, rather than a single arbitrary model, is
obtained. If all the A's and α's are known the λ_{ij} are uniquely
determined.

The key point in this method is the formulation of a gen-
erating model incorporating all the invariants of the data and a
set of variables equal in number to the degrees of freedom remaining
for the system. Then all possible models that are consistent with
the measurement can be obtained from the generating model by proper
mapping operations in which the invariants are preserved.

Practical applications of this method have been made by
several investigators (39, 40). But still the basic problem as to
how many exponentials are necessary to fit a set of data remains to

be resolved. The biological identification of compartments also offers a considerable problem.

Modified Compartmental Analysis

In view of the present knowledge of the details of organ structure and function, and with the current scarcity of good data for diffusion coefficients and membrane permeabilities of various substances in the various spaces, it would be wise to choose models which minimze the need for detailed information while still retaining sufficient realism to simulate the phenomena of interest. Therefore, most models ignore diffusion within the extracellular spaces and assume that these regions are well mixed. Thus, the resistance to transfer is only associated with transport across the membrane and with a barrier to transfer at the tissue surface, if any.

Perhaps the most difficult condition to fulfill for the compartmental analysis is the condition that the tracer be distributed uniformly throughout the compartments concerned. If the time of mixing is about the same order of magnitude as the rate of transfer across the barrier between the compartments or if the viscosity of the fluid in a compartment is high, it is clear that special attention must be paid to the assumption of uniform distribution.

There will always be diffusion effects that must be considered when a tracer moves through a compartment and it is necessary to insure either that the diffusion effects are small compared

to the transfer rate or that special terms are introduced to the
equations to take account of these effects. The diffusion effects
become important especially when a whole muscle tissue is used for
the kinetic study of ion exchange. It has been noted by several
investigators that the rate of transfer depends upon the dimension
of the sample tissue (25, 35). This indicates that diffusion plays
at least some part in the process, limiting the equilibration between
the external medium and the extracellular space, because the basic
permeability equation only involves the volume/surface area ratio of
the cells and not the size of the tissue when several or many cells
are examined together.

In compartmental analysis, if the cellular membrane is rate
limiting and the cells are assumed to be a single compartment, a
single exponential should describe the washout. Studies conducted
on sodium washout from smooth muscles have indicated that the
process does not approach a single exponential under the experimental
conditions (21, 24, 39). The mathematical description of such
curves requires more than two exponential functions needed for a
simple model based on an extracellular and an intracellular
compartment.

Therefore more realistic, though involved, mathematical
approaches which describe diffusion of the tracer in the extra-
cellular compartment are needed. In other words, the kinetics of
the transfer of ions between an assembly of cells and the surround-
ing medium depend on two factors, the rate of diffusion of the ion
in the extracellular space and the rate of crossing the cell

boundaries. This differes from a straight compartmental analysis by the consideration of the diffusion process. The closest compartmental model would account for this diffusive resistance by the inclusion of a "permeable barrier" between a well mixed extracellular space and the washing solution.

As mentioned earlier, many uncertainties still exist concerning the nature of the intracellular space. The assumption of a uniform intracellular electrolyte pool made in membrane models has been challenged by many investigators, who put more emphasis on bulk properties of the cytoplasm than on the membrane properties in the interpretation of cellular permeability (8, 37). In recent work the association-induction hypothesis has been further developed to account for quantitative aspects of ion permeability and selective accumulation (38).

According to this model the ions in the cell exist in two states, either dissolved in cell water or associated with fixed sites. The entrance of ions into such a cell would take place via two routes: diffusion through channels of cell water or adsorption-desorption to fixed charges, membrane being considered as part of the cytoplasmic phase. The ion exchange process, therefore, is treated as the sum of a diffusion process through the cell water as well as the extracellular space and a rate process of adsorption-desorption at the fixed, charged sites.

Jones (33) applied this model for interpreting the ion exchange properties of the vascular wall. His results indicated that more sodium ions were exchanged with diffusion kinetics than

were contained in the extracellular space and the excess could not be attributed to connective tissue adsorption. Thus a membrane model appeared to be inadequate to describe the data. The uncertainties concerning the nature of tissue compartments and the ion distribution in the tissue, however, render his interpretation doubtful. Furthermore, current accumulation of evidence favors the membrane model for interpreting kinetic data on biological tissues.

In this work, the kinetics of transport of sodium ions in arterial walls were studied using the tracer washout technique. The experimental washout data were then interpreted based on the membrane concept. A mathematical model (involving diffusion in the extracellular space and transport across the cell membranes by both passive and active mechanisms) was developed and used for the analysis of the washout data.

IV. EXPERIMENTAL METHODS

The transport of sodium ions in arteries was studied both experimentally and theoretically. The experimental results were then used to test a mathematical model which takes into account diffusion in the extracellular space and transport across cell membranes by passive and active mechanisms.

Experimental Approach

In general, the methods which have been used in the past to study transport of ions in vascular tissue have involved the washout of tagged ions from strips of tissue cut in a helical manner from large arteries. These studies have usually been conducted with the tissue relaxed rather than under tension. In this work we have altered the previous procedures such that sections of artery (rather than strips) under tension could be used.

Sections of a small branch of the femoral artery were removed from mongrel dogs weighing 20 to 30 kg, which were anesthetized by intravenous injection of sodium pentobarbital (33 mg/kg).

The artery was mounted on a section of stainless steel rod slightly larger than the inside diameter of the vessel (Figure 5). In this manner the artery could be held rigid and under tension throughout the experiment to simulate as closely as possible physiologic conditions.

Figure 5.--Cutaway view of tissue as mounted on stainless steel.

SECTION OF ARTERY

STAINLESS STEEL ROD

EXTRACELLULAR SPACE

SMOOTH MUSCLE CELLS

b

a

Na^{22} FREE

WASHING SOLUTION
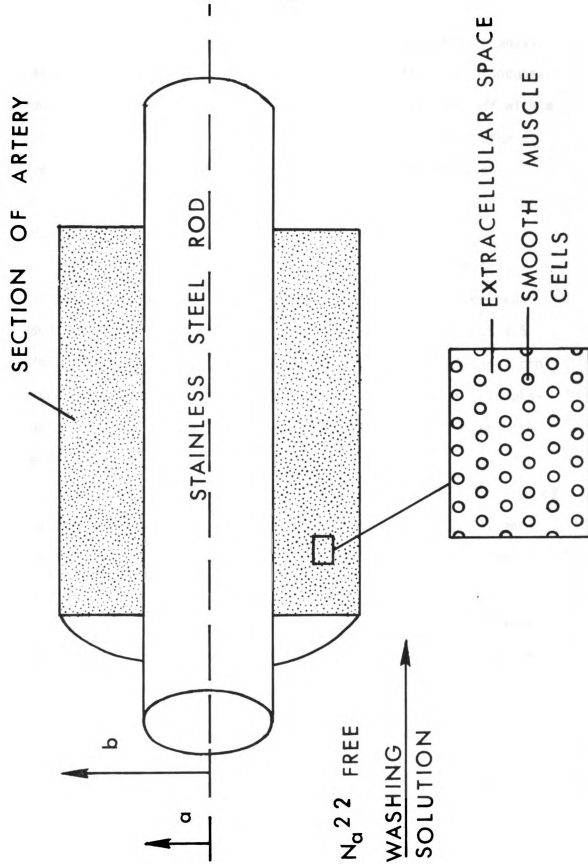
The artery mounted on the rod was then incubated in physiologic Ringer's solution for 30 minutes. After this first incubation the tissue was cleaned and loose adventitia trimmed off with a small scissors. The length and outside diameter of the tissue at several locations were measured using a microcomparator and averaged, the inside diameter being determined by the size of the rod.

The tissue was again incubated in physiologic Ringer's solution. This time radioactive Na^{22} as NaCl, carrier-free, was added to the incubating solution at a concentration of about 1.5 $\mu c/ml$ ($\sim 10^{-3}$ mM/1), which was not enough to alter the chemical concentration but sufficient to give reasonable count rates. Incubation periods of 90 minutes were used to insure equilibration with the Na^{22} (21).

The experimental incubation was carried out in about 5 ml of physiologic Ringer's solution bubbled with 95% O_2 and 5% CO_2 and maintained at 37°C or room temperature (21 ± 2°C) depending on the experiment.

Ringer's solutions were prepared from distilled deionized water and analytical reagent grade chemicals. The composition in mEq/1 was as follows:

NaCl	= 123.0	Calcium Gluconate	= 4.8
$NaHCO_3$	= 23.0	$MgCl_2$	= 2.0
KCl	= 4.2	Glucose	= 1 g/1

giving a Na^+ concentration of 146 mEq/1 and a K^+ concentration of 4.2 mEq/1. Ringer's solutions having four different K^+

concentrations--normal, half of the normal, one-quarter of the normal, and K^+-free--were used to investigate the effects of lowering potassium level on the kinetics of Na^+ transfer in the artery.

After the second incubation to equilibrate the tissue with Na^{22}, the tissue mounted on the rod was removed from the incubating solution and slightly blotted on tissue paper to clean the residual external fluid on the surface of the tissue. The area of the rod not covered with the tissue was also carefully washed with distilled water to avoid possible error in measuring the initial count rate. The rod with mounted tissue was then inserted into the washing chamber and the chamber was placed in the well of a 3" NaI crystal detector (Figure 6). Figure 7 shows details of the washing chamber.

The Na^{22} in the tissue was then washed continuously with untagged Ringer's in an apparatus designed to maintain constant temperature and constant flow throughout the entire washing period. A schematic is shown in Figure 8. In a large glass jar 15 liters of Ringer's solution were made and continuously bubbled with a gas mixture of 95% O_2 and 5% CO_2 and held at constant temperature. This Ringer's solution was pumped through the chamber, washing the surface of the artery with untagged solution. Constant flow was maintained with a pump. The Ringer's solution was pumped in such a way that the solution flowed upwards in the region of the chamber where the tissue was located. The bypass arrangement allowed setting the apparatus at working condition before starting the washing of the tissue.
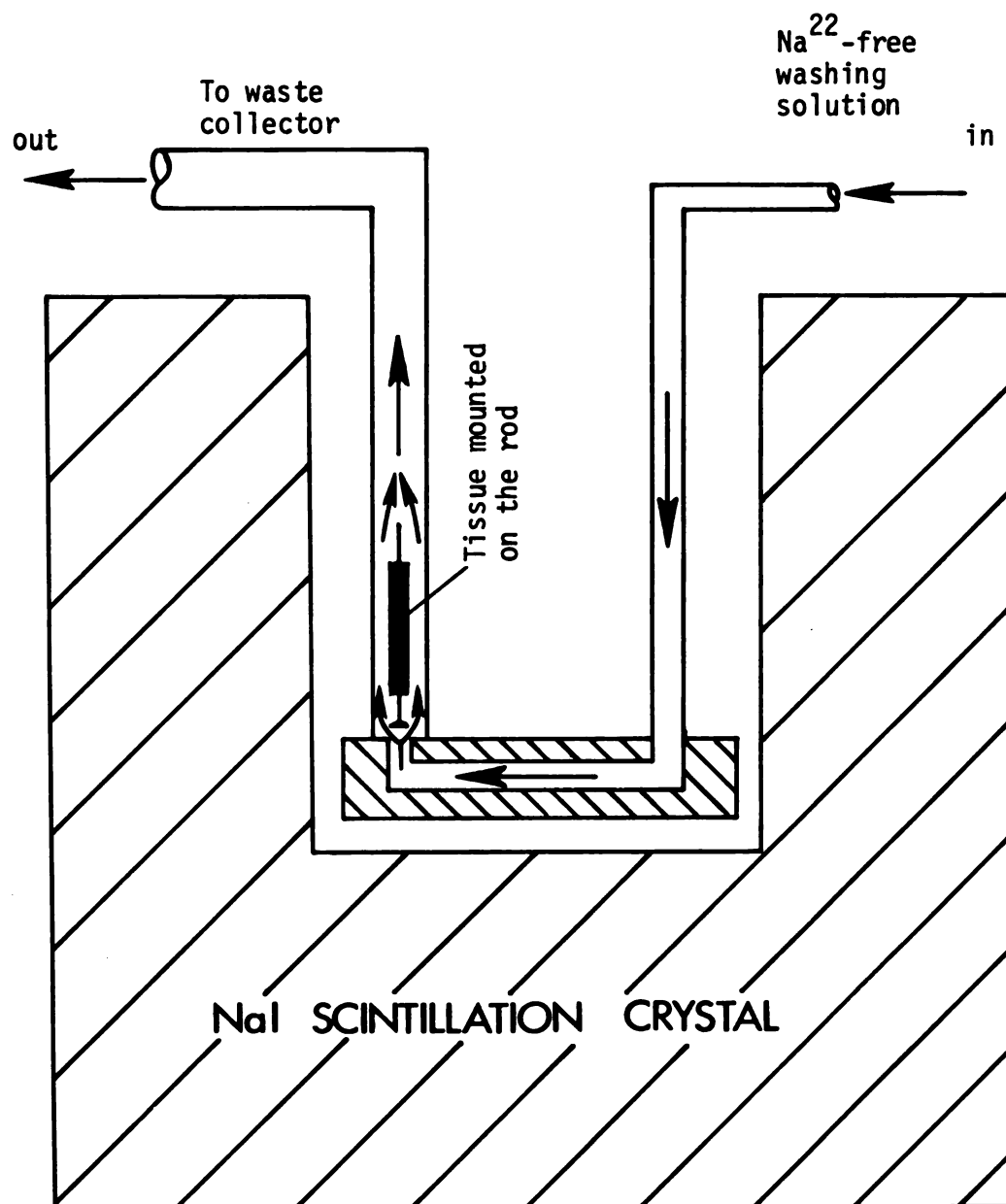
Figure 6.--Diagram of the washing chamber with the tissue mounted on the rod and placed in the NaI detector crystal.
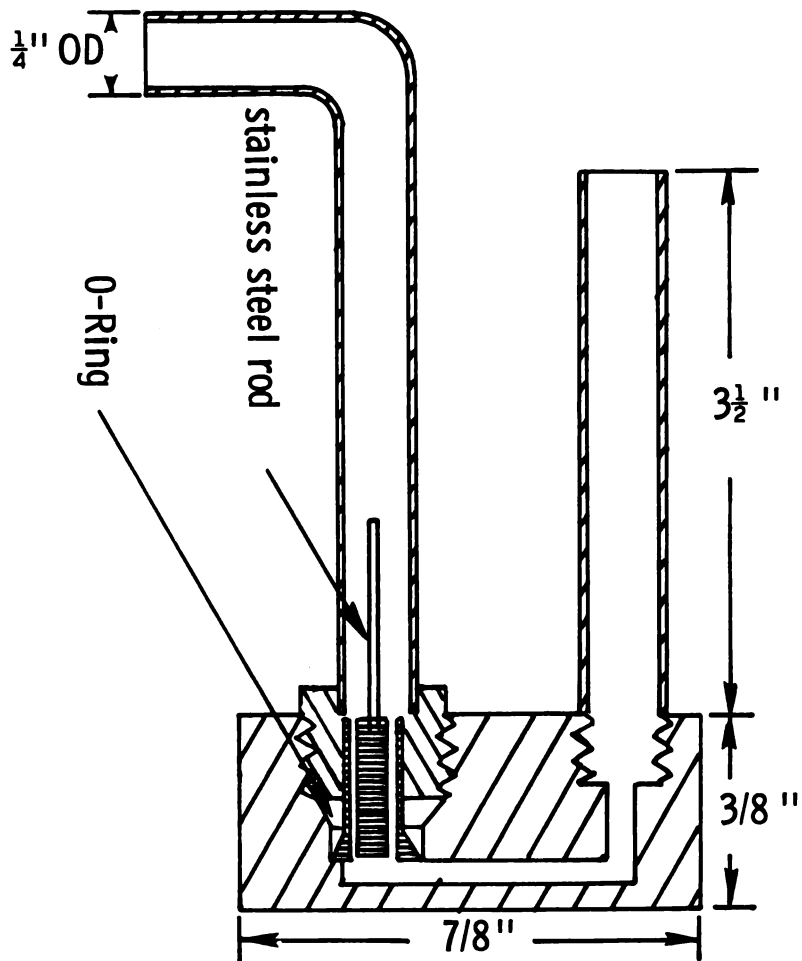
Figure 7.--Details of the washing chamber with the stainless steel rod.
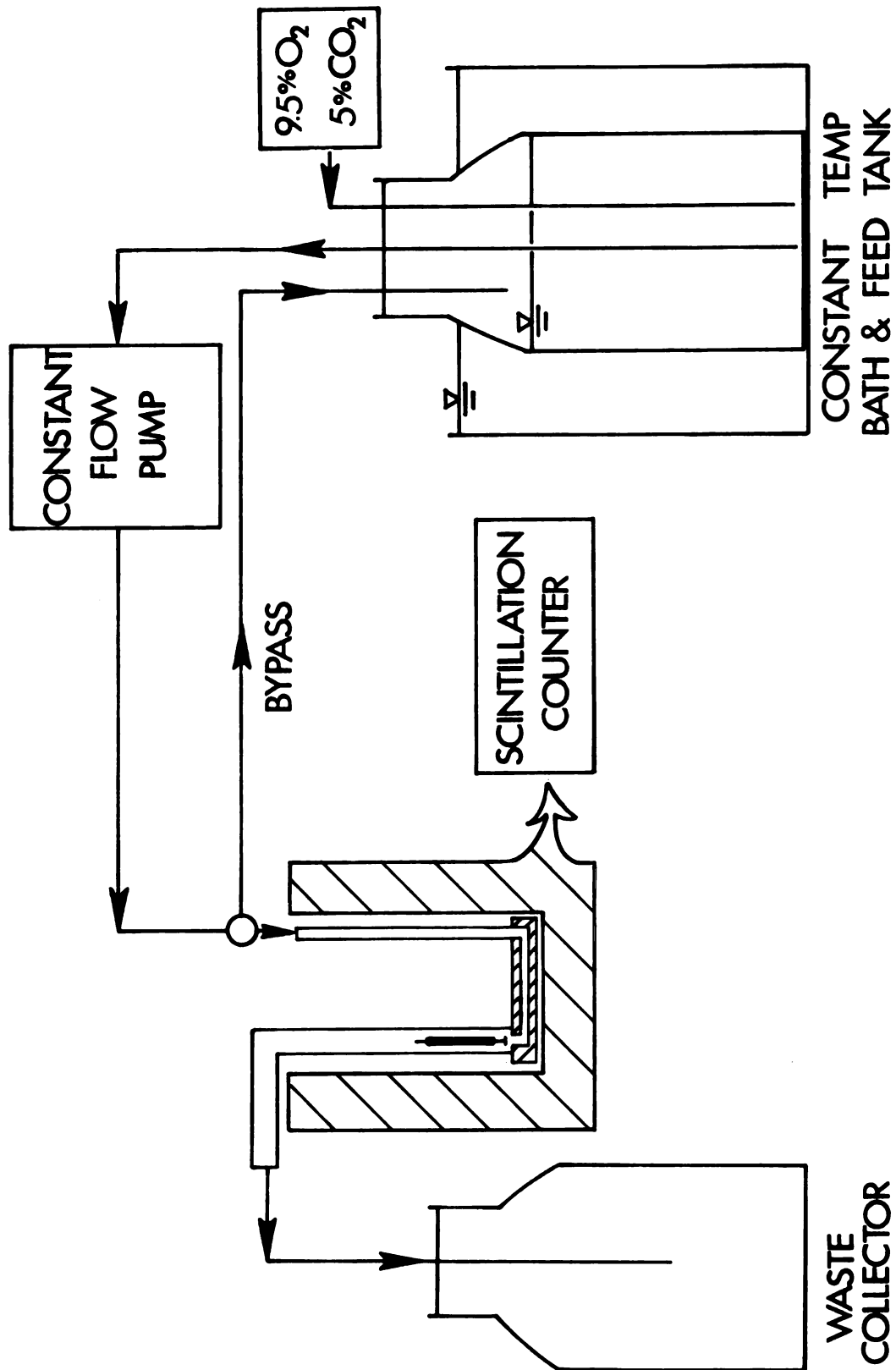
Figure 8.--Flow diagram of the washout experiment.

The internal volume of the chamber between the location of the tissue and the flow outlet was 0.4 ml and the flow rate was 3.0 ml/sec. Thus the residence time of Na^{22} was in the order of 0.13 sec after diffusing from the tissue. It was assumed that any mass transfer resistance at the outside surface of the tissue could be neglected at these flow conditions.

During the washout period the total radioactivity remaining in the tissue was monitored by counting for fixed time intervals. Figure 9 shows the arrangement of electronic instruments for measuring the radioactivity in the tissue. The system permitted the use of counting intervals as low as 1.0 second and by using two scalers this interval was changeable during a run without interrupting the current counting period. Thus the fast initial washing away of Na^{22} could be recorded for short times, which was essential for determining initial differential count rate. The total wash period was approximately 45 minutes. Longer periods did not appear desirable as the lower count rates at later times resulted in poor statistics.

After the washing period, the washing chamber without the tissue was counted as a background and this was subtracted from the original values. The net count rates were then plotted on a semilog paper with linear time axis.

Determination of Initial Count Rate

Defining instantaneous count rate of the tissue at any time, t to be $N^*(t)$, integral counts up to time t, $\bar{N}^*(t)$ becomes

57
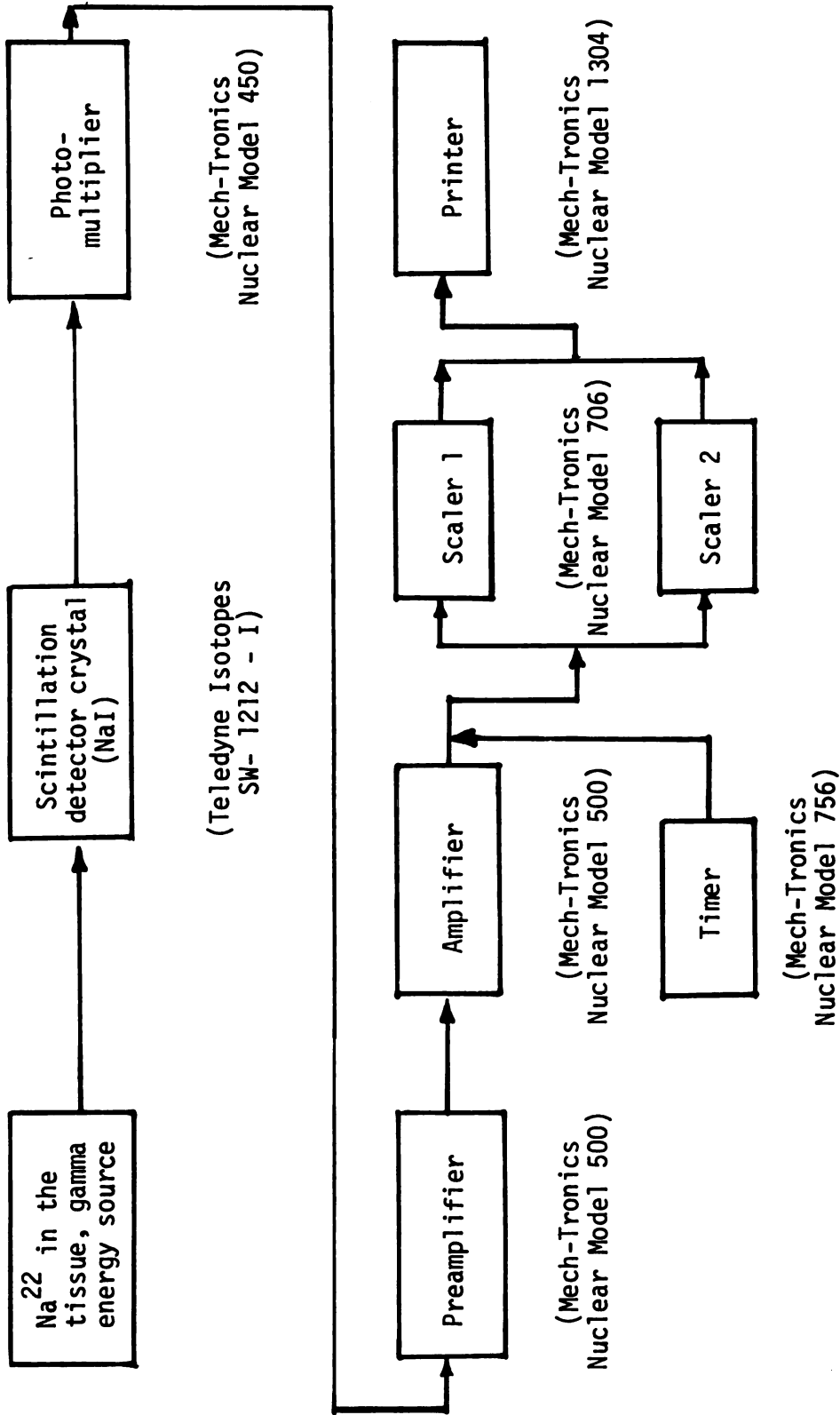
Figure 9.--Block diagram of the process of measuring the radioactivity in the tissue.

$$\bar{N}^*(t) = \int_0^t N^*(t) \cdot dt \tag{12}$$

Since $N^*(t)$ is the summed effects of radioactivities in the extra- and intracellular spaces, it can be expressed as follows:

$$N^*(t) = N_e^*(t) + N_i^*(t) \tag{13}$$

where $N_e^*(t)$ and $N_i^*(t)$ are instantaneous count rates due to the radioactivities in the extra- and intracellular spaces, respectively. Thus,

$$\bar{N}^*(t) = \int_0^t (N_e^*(t) + N_i^*(t)) dt \tag{14}$$

or

$$= N_e^*(0) \left[\int_0^t \frac{N_e^*(t)}{N_e^*(0)} dt + \int_0^t \frac{N_i^*(t)}{N_e^*(0)} dt \right] \tag{15}$$

where $N_e^*(0)$ is the initial value of $N_e^*(t)$. For very small times, the fluxes across the cell membranes would be negligible and the term $N_i^*(t)/N_e^*(0)$ can be approximated as follows:

$$\frac{N_i^*(t)}{N_e^*(0)} \simeq \frac{N_i^*(0)}{N_e^*(0)} \simeq \text{constant} \tag{16}$$

where $N_i^*(0)$ is the initial value of $N_i^*(t)$. With the assumption that there is no loss of cellular tag for very small times, $N_e^*(t)/N_e^*(0)$ can be expressed in terms of the sodium[22] which has left the extra-cellular space:

$$\frac{N_e^*(t)}{N_e^*(0)} = 1 - \frac{M_t}{M_0} \tag{17}$$

where M_0 is the initial amount of the sodium[22] and M_t the amount which has diffused from the extracellular space at time t.

Defining the number of moles of sodium[22] which has left the tissue per unit external surface area at any time to be $n(t)$,

$$\frac{M_t}{M_0} = \frac{n(t) \, A}{C_{Na,e}^*(0) V_t (V_e/V_t)} \tag{18}$$

where A is the total surface area of the tissue, $C_{Na,e}^*(0)$ the initial extracellular sodium[22] concentration, V_t the volume of the tissue, and V_e the extracellular volume. Rearranging Equation (18) gives

$$n(t) = C_{Na,e}^*(0) \left[\frac{V_t}{A}\right] \left[\frac{V_e}{V_t}\right] \left[\frac{M_t}{M_0}\right] \tag{19}$$

For very small times, diffusion process would affect only the region very close to the surface. Therefore $n(t)$ can be assumed to remain the same regardless of the tissue geometry. Crank (16) has shown that for the solid cylindrical geometry, M_t/M_0 becomes:

$$\frac{M_t}{M_0} = \frac{4}{\pi^{1/2}} \left[\frac{Dt}{b^2}\right]^{1/2} - \frac{Dt}{b^2} - \frac{1}{3\pi^{1/2}} \left[\frac{Dt}{b^2}\right]^{3/2} + \cdots \tag{20}$$

The substitution of this equation for M_t/M_0 in Equation (19) gives

$$
n(t) = C^*_{Na,e}(0) \left(\frac{b}{2}\right) \left(\frac{V_e}{V_t}\right) \left[\frac{4}{\pi^{1/2}} \left(\frac{Dt}{b^2}\right)^{1/2} - \frac{Dt}{b^2} \right.
$$

$$
\left. - \frac{1}{3\pi^{1/2}} \left(\frac{Dt}{b^2}\right)^{3/2} + \cdots \right] \tag{21}
$$

where b is the radius of the cylinder. For the tissue in hollow cylindrical geometry with inner surface insulated, we have

$$
\frac{A}{V_t} = \frac{2b}{b^2 - a^2} \tag{22}
$$

where b is the outer radius and a the inner radius. Substituting Equations (21) and (22) into Equation (18) gives

$$
\frac{M_t}{M_0} = \left(\frac{b^2}{b^2 - a^2}\right) \left[\frac{4}{\pi^{1/2}} \left(\frac{Dt}{b^2}\right)^{1/2} \right.
$$

$$
\left. - \frac{D}{b^2} t - \frac{1}{3\pi^{1/2}} \left(\frac{Dt}{b^2}\right)^{3/2} + \cdots \right] \tag{23}
$$

Combining Equation (23) and Equation (17) gives

$$
\frac{N^*_e(t)}{N^*_e(0)} = 1 - \left(\frac{b^2}{b^2 - a^2}\right) \left[\frac{4}{\pi^{1/2}} \left(\frac{Dt}{b^2}\right)^{1/2} \frac{D}{b^2} t \right.
$$

$$
\left. - \frac{1}{3\pi^{1/2}} \left(\frac{Dt}{b^2}\right)^{3/2} + \cdots \right] \tag{24}
$$

Substituting Equations (24) and (16) into Equation (15) gives

$$\bar{N}^*(t) = [N_i^*(0)+N_e^*(0)] \cdot t - N_e^*(0) \cdot \left[\frac{b^2}{b^2 - a^2}\right] \cdot \left[\frac{8}{3}\left(\frac{D}{\pi b^2}\right)\right]^{1/2}$$

$$\cdot t^{3/2} - \frac{D}{2b^2} \cdot t^2 - \left(\frac{2}{15}\right)\left(\frac{D^3}{b^6}\right) \cdot t^{5/2} + \cdots \right] \quad (25)$$

Dividing both sides with t,

$$\frac{\bar{N}^*(t)}{t} = N^*(0) - N_e^*(0) \cdot \left[\frac{b^2}{b^2 - a^2}\right] \cdot \left[\frac{8}{3}\left(\frac{D}{\pi b^2}\right)\right]^{1/2} \cdot t^{1/2} - \frac{D}{2b^2} \cdot t$$

$$- \left(\frac{2}{15}\right)\left(\frac{D^3}{\pi b^6}\right) \cdot t^{3/2} + \cdots \right] \quad (26)$$

On plotting $\bar{N}^*(t)/t$ vs $\sqrt{t}$, the intercept becomes the initial instantaneous count rate, the terms greater than $\sqrt{t}$ being neglected (see Figure 10).

In this work, the activities were measured at 3 second intervals for the first 30 seconds. Integrated data up to 18 seconds were then used to determine the initial instantaneous count rate, $N^*(0)$.

Theoretical Description of the Washout Process

A short section of artery, mounted on a stainless steel rod, is assumed to be made up of a collection of smooth muscle cells which exchange solutes with the extracellular fluid. The solutes can in turn diffuse in the extracellular space and exchange with the

The figure shows $\frac{\bar{N}^*(t)}{t}$ plotted against $\sqrt{t}$, sec. The dashed line extrapolates to the intercept.

intercept = $N^*(0)$

slope = $N_e^*(0) \left[\frac{b^2}{b^2-a^2}\right]\left[\frac{8}{3}\right]\left[\frac{D}{\pi b^2}\right]^{1/2}$
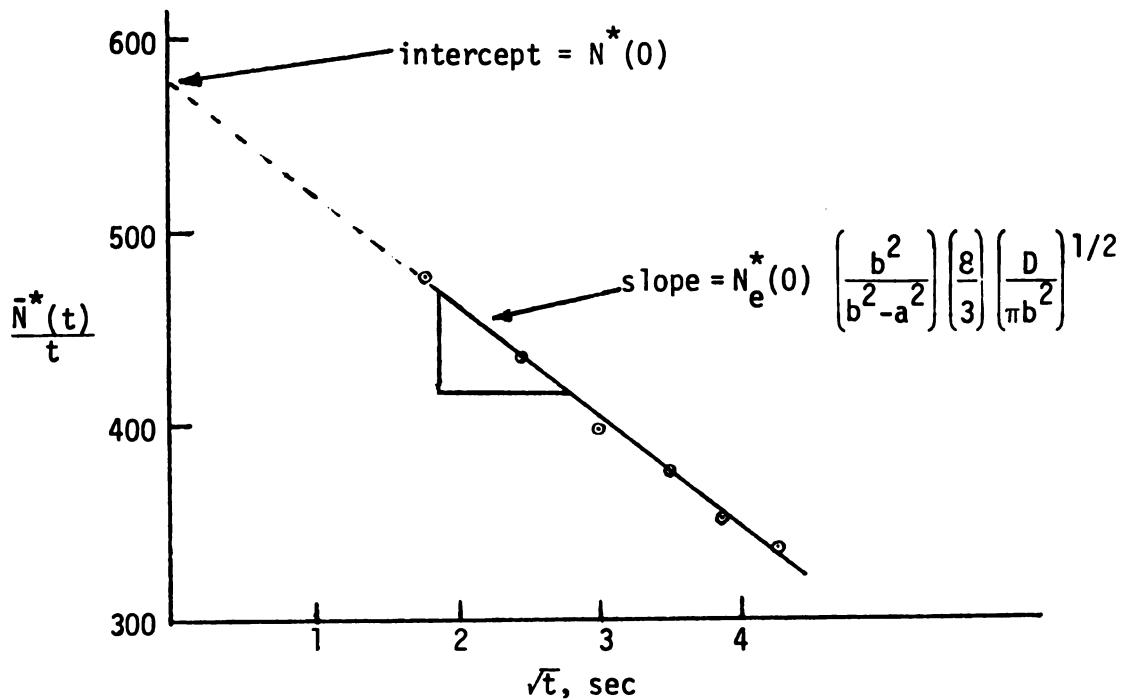
Figure 10.--Graphical representation of the determination of initial count rate.

washing solution at the outer surface of the tissue. Figure 5 is a view of the tissue with the appropriate dimensions labeled.

The Ion Fluxes Across Membranes of Vascular Smooth Muscle Cells

In vascular smooth muscles under steady state, there is a net passive influx of sodium ions across cell membranes, which is balanced by an active transport of sodium ions out of the cells. Since the thickness of the membrane (75 Å) is negligible compared to the other cellular dimensions, the membrane can be assumed to be planar with constant thickness, and to be infinite in extent in

the transverse plane. This assumption validates a one-dimensional treatment of ion flux (see Figure 11) across the membrane.


```
              +  |    |  -
              +  |    |  -
              +  |    |  -
    Extra-    +  |mem-|  -   Intra-
    cellular  +  |brane| -   cellular
    space     +  |    |  -   space
              +  |    |  -
              +  |    |  -
              +  |    |  -
  _____|____|_____ x
              0        d
```
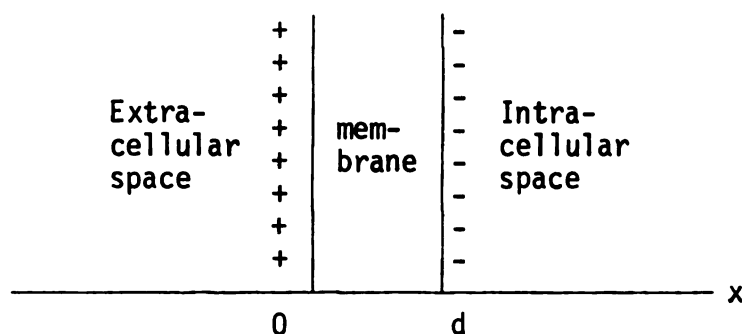
Figure 11.--The planar membrane model.

There are two major forces which produce a passive diffusional movement of sodium ions across the cell membranes: chemical concentration gradient and transmembrane potential gradient. The flux of sodium ion resulting from concentration gradient (∇C_{Na}) is described by Fick's 1st law as

$$j_{Na,dif} = -D_{Na} \nabla C_{Na} \tag{27}$$

where D_{Na} is the diffusion coefficient of the sodium ion. The flux of sodium due to the electrical force (electrical potential gradient, ∇E_m), which is present across the membrane, becomes

$$j_{Na,el} = -u_{Na} \frac{z_{Na}}{|z_{Na}|} C_{Na} \cdot \nabla E_m \tag{28}$$

where u_{Na} is the sodium ion mobility. The factor $z_{Na}/|z_{Na}|$ takes care of the sign of the ion flux, which is in the direction of the

negative gradient for cations and in the opposite direction for anions (for sodium ions this ratio becomes unity). The total fluxes due to the sum of the concentration gradient and the electric force are then

$$j_{Na} = -D_{Na} \cdot \nabla C_{Na} - u_{Na} \, C_{Na} \cdot \nabla E_m \qquad (29)$$

With the use of the Einstein relation (45), the mobility can be expressed in terms of diffusion coefficient as

$$u_{Na} = \frac{D_{Na}F}{RT} \qquad (30)$$

If Equation (30) is substituted for u_{Na}, Equation (29) becomes

$$j_{Na} = -D_{Na} \left(\nabla C_{Na} + \frac{F}{RT} \cdot C_{Na} \cdot \nabla E_m \right) \qquad (31)$$

The units of j_{Na} are moles per unit area per unit time.

In order to solve this equation for j_{Na} (constant in the steady state) it is necessary to know either the concentration profile or the electrical potential profile within the membrane as well as the Na ion partition coefficients of the membrane at both sides.

Goldman (23) made the assumption that the electrical field within the cell membrane is constant. In this case the electrical potential increases linearly through the membrane and

$$\nabla E_m = \frac{dE_m}{dx} = \frac{E_m}{d} \qquad (32)$$

where x represents position in the membrane and d is the membrane thickness (see Figure 11). With these assumpsions, Equation (31) becomes

$$j_{Na} = - D_{Na} \nabla C_{Na} - \frac{D_{Na} E_m F}{RTd} C_{Na} \tag{33}$$

This is an ordinary first-order separable differential equation where the dependent variable is the concentration C_{Na} and the independent variable is x. Rearranging gives

$$\frac{dC_{Na}}{dx} + \left(\frac{E_m F}{RTd}\right) C_{Na} = - \frac{j_{Na}}{D_{Na}} \tag{34}$$

and solving for C_{Na} as a function of x yields

$$C_{Na} = N \exp \left[-\left(\frac{E_m F}{RTd}\right) x\right] - \frac{j_{Na} RTd}{D_{Na} E_m F} \tag{35}$$

where N is a constant of integration.

The boundary conditions are

$$x = 0 \qquad\qquad C_{Na} = C_{Na,0} \tag{36a}$$

$$x = d \qquad\qquad C_{Na} = C_{Na,d} \tag{36b}$$

With the boundary condition at x = 0, the integration constant N is evaluated as

$$N = C_{Na,0} + \frac{j_{Na} RTd}{D_{Na} E_m F} \tag{37}$$

Substituting Equation (37) into Equation (35) gives

$$C_{Na} = \left[C_{Na,0} + \frac{j_{Na}RTd}{D_{Na}E_{m}F} \right] exp \left[-\frac{E_{m}F}{RTd} \cdot x \right] - \frac{j_{Na}RTd}{D_{Na}E_{m}F} \tag{38}$$

It can be seen that the concentration of sodium ion in the membrane is dependent upon surface concentrations, net flux of the sodium ion, and the transmembrane potential difference.

By applying the boundary condition at $x = d$ and solving for j_{Na}, one gets

$$j_{Na} = \left[\frac{\frac{D_{Na}E_{m}F}{RTd} exp \left[-\frac{E_{m}F}{RT} \right]}{1 - exp \left[-\frac{E_{m}F}{RT} \right]} \right] C_{Na,0} - \left[\frac{\frac{D_{Na}E_{m}F}{RTd}}{1 - exp \left[-\frac{E_{m}F}{RT} \right]} \right] C_{Na,d} \tag{39}$$

Next it is assumed that the concentrations of the sodium ion at the surfaces of the membrane are related to the concentrations in the bulk fluids bathing the membrane by a constant β, called the partition coefficient (assumed equal on both sides of the membrane):

$$C_{Na,0} = \beta \, C_{Na,e} \tag{40a}$$

$$C_{Na,d} = \beta \, C_{Na,i} \tag{40b}$$

where $C_{Na,e}$ and $C_{Na,i}$ represent the sodium concentrations in the extracellular fluid and the intracellular fluid, respectively. By applying the partition coefficient assumption and defining the membrane permeability to sodium ion (P_{Na}) to be

$$P_{Na} = \frac{D_{Na}\beta}{d}$$

the flux Equation (39) becomes

$$j_{Na} = \frac{P_{Na}(-E_m)F\ C_{Na,e} - P_{Na}(-E_m)F\ \exp\ (E_mF/RT)\ C_{Na,i}}{RT\ [1 - \exp\ (E_mF/RT)]} \qquad (41)$$

This is the widely used constant field equation for the net passive flux for sodium ion across the cell membrane. If we define K_1 and K_2' as follows,

$$K_1 = \frac{P_{Na}\ (-E_m)F}{RT\ [1 - \exp\ (E_mF/RT)]} \qquad (42)$$

$$K_2' = \frac{P_{Na}\ (-E_m)F\ \exp\ (E_mF/RT)}{RT\ [1 - \exp\ (E_mF/RT)]} \qquad (43)$$

then,

$$j_{Na} = K_1\ C_{Na,e} - K_2'\ C_{Na,i} \qquad (44)$$

The passive flux of Na^{22} then can be taken as the product of the total passive efflux and the intracellular specific activity with a similar term for the influx. Thus, the net passive flux of sodium[22] per unit area per unit time becomes

$$j_{Na}^* = K_1\ C_{Na,e} \left(\frac{C_{Na,e}^*}{C_{Na,e}}\right) - K_2'\ C_{Na,i} \left(\frac{C_{Na,i}^*}{C_{Na,i}}\right) \qquad (45)$$

or

$$= K_1\ C_{Na,e}^* - K_2'\ C_{Na,i}^* \qquad (46)$$

If we define the active efflux of total sodium across the cell membrane per unit area per unit time (active pumping rate) to be S, the active efflux of Na^{22} becomes

$$j^{*}_{Na,a} = S \cdot \left(\frac{c^{*}_{Na,i}}{c_{Na,i}} \right) \tag{47}$$

Since the specific activities of Na^{22} in both the extra- and intracellular fluids change while the tissue is being washed, the net flux of Na^{22} is not zero but becomes

$$j^{*}_{T} = K_1 \, c^{*}_{Na,e} - \left[K'_2 + \frac{S}{c_{Na,i}} \right] c^{*}_{Na,i} \tag{48}$$

Since S and $c_{Na,i}$ are both constant during an experiment, Equation (48) can be written as follows

$$j^{*}_{T} = K_1 \, c^{*}_{Na,e} - K_2 \, c^{*}_{Na,i} \tag{49}$$

where

$$K_2 = K'_2 + S/c_{Na,i}$$

According to Plonsey (19), the constant field approximation is fairly good for biological membranes and exact if the permeable ions are univalent and if the total ionic concentrations on each side of the membrane are equal. Zellman and Shi (59) also tested the constant field assumption, concluding that the constant field flux equation is very good for biological membranes and is the best available approximation of the ionic fluxes.

There are no theoretical considerations which indicate that the partition coefficient on one side of a membrane would be unequal to the partition coefficient on the opposite side of the membrane. On the contrary, if the ions are passively diffusing through the membrane, the partition coefficients would be expected to be equal.

The constant field flux equation, therefore, is not only a good approximation but is also the best ionic flux equation presently available. An important criticsm of the constant field flux equation is that the permeability coefficients are not obtainable from fundamental microscopic membrane properties but rather are inferred from the overall behavior.

The Washout Process

During the washout period, sodium-22 diffuses from the extracellular space to the washing solution and is carried away. Since the thickness of the tissue used for the experiments was very small compared to the length, the diffusion process is assumed to occur only in the radial direction without an end effect.

If we write a conservation equation for the extracellular Na^{22}, we obtain

$$\frac{\partial C_{Na,e}^{*}}{\partial t} = D \left(\frac{\partial^{2} C_{Na,e}^{*}}{\partial r^{2}} + \frac{\partial C_{Na,e}^{*}}{\partial r} \right) + \frac{\varepsilon_{i}}{\varepsilon_{e}} a \left(K_{2} C_{Na,i}^{*} - K_{1} C_{Na,e}^{*} \right) \quad (50)$$

where $C_{Na,e}^{*}$ and $C_{Na,i}^{*}$ are the extra- and intracellular concentrations of the Na^{22} ions at a radial position r, respectively; D is the effective diffusion coefficient in the extracellular space;

ϵ_i and ϵ_e are the respective volume fractions of the tissue; K_1 and K_2 are mass transfer coefficients for influx and efflux of the Na^{22} ion; and $\underline{a}$ is the cell membrane area per unit volume of intracellular fluid. Also, writing a conservation equation on intracellular fluid:

$$\frac{\partial C^*_{Na,i}}{\partial t} = a\ (K_1 C^*_{Na,e} - K_2 C^*_{Na,i}) \tag{51}$$

When the tissue gets equilibrated with the sodium^{22} ions the specific activities in the extra- and intracellular fluids become equal to each other:

$$\frac{C^*_{Na,e}(0)}{C_{Na,e}} = \frac{C^*_{Na,i}(0)}{C_{Na,i}} \tag{52}$$

where $C^*_{Na,e}(0)$ and $C^*_{Na,i}(0)$ are the initial concentrations in the extra- and intracellular spaces, respectively, before the washing takes place. Rearranging Equation (52) gives

$$\frac{C^*_{Na,i}(0)}{C^*_{Na,e}(0)} = \frac{C_{Na,i}}{C_{Na,e}} \tag{53}$$

Since the tissue is in a steady state with respect to overall sodium concentration, the concentration ratio, $C_{Na,i}/C_{Na,e}$, remains constant. This ratio is defined to be ϕ:

$$\frac{C^*_{Na,i}(0)}{C^*_{Na,e}(0)} = \phi \tag{54}$$

Then, the initial differential count rate, $N^*(0)$, obtained from the experimental result, becomes

$$N^*(0) = BV_t [\varepsilon_i C^*_{Na,i}(0) + \varepsilon_e C^*_{Na,e}(0)] \tag{55}$$

where B is a proportionality constant which relates the total Na^{22} ions to their count rate. Henceforth, this proportionality constant is incorporated into the concentration terms. That is, the concentrations, $C_{Na,e}$ and $C^*_{Na,i}$, are treated as actual count rates equivalent to the concentrations.

Since the tissue mounted on a stainless steel rod is washed on the outer surface there is no flux across the inner surface. Also with a flow rate of 3.0 ml/sec through the space of about 0.4 ml any mass transfer resistance at the outer surface of the tissue can be neglected.

Thus, the initial and boundary conditions become:

$$C^*_{Na,e} = C^*_{Na,e}(0) \tag{56}$$

$$t = 0$$

$$C^*_{Na,i} = C^*_{Na,i}(0) \tag{57}$$

$$\frac{\partial C^*_{Na,e}}{\partial r} = 0 \qquad r = a \tag{58}$$

$$C^*_{Na,e} = 0 \qquad r = b \tag{59}$$

The values of $C_{Na,e}^*(0)$ and $C_{Na,i}^*(0)$ are obtained by solving Equations (54) and (55) simultaneously:

$$C_{Na,e}^*(0) = \frac{N^*(0)}{V_t(\varepsilon_i \cdot \phi + \varepsilon_e)} \tag{60}$$

$$C_{Na,i}^*(0) = \phi \cdot C_{Na,e}^*(0) \tag{61}$$

Equations (50) and (51) were solved numerically using the Crank-Nicolson method (14) to give $C_{Na,e}^*$ and $C_{Na,i}^*$ in the tissue as functions of radial position and time. The total instantaneous count rates of Na^{22} ions at any time, t, $N^*(t)$ is, then, given by

$$N^*(t) = \int_a^b 2\pi rL(C_{Na,i}^* \cdot \varepsilon_i + C_{Na,e}^* \cdot \varepsilon_e)dr \tag{62}$$

Equation (62) was integrated numerically, using the results of the above simulation.

Since the experimental data from the washout are integral counts over specific time intervals, $N^*(t)$ must be integrated over the appropriate counting intervals in order to simulate the experimental values of $\bar{N}^*(t)$:

$$\bar{N}^*(t) = \int_{t-\Delta t}^t N^*(t) \, dt \tag{63}$$

Again, this integration was carried out numerically using the computer.

Thus for a given choice of parameters $(D, K_1, K_2, \varepsilon_i, \varepsilon_e, \phi)$ in the model, washout curves were simulated and compared to the experimental data. The parameters were then adjusted until a fairly good fit of the data was obtained. Then using these values as the initial guess, the parameters were finally optimized with the use of the KINFIT program (19).

In order to minimize the number of parameters to be adjusted, ε_i, ε_e, and E were chosen, a priori, based on the best estimates available in the literature. The extracellular space $(\varepsilon_e = 0.4)$ was based on the measurements of Villamil et al. (56) on canine carotid artery using sucrose-C^{14}. The intracellular space $(\varepsilon_i = 0.37)$ was estimated from the urea-C^{14} uptake measurements by Arvil et al. (2) and the total water content of canine carotid artery (33, 56). a was taken to be 10^4 cm^2/cm^3 based on a smooth muscle cell radius of 2×10^{-4} cm (33). The membrane potential (E = -57 mV) was based on the measurements by Hendrickx and Casteels (27) on the ear artery of the rabbit. We also obtained a value close to this (~55 mV) from a preliminary study of the membrane potential of vascular smooth muscle in canine arteries. The diffusion coefficient was adjusted only through the preliminary optimizing process for the 12 control runs at 37°C and 4 runs at room temperature. The 12 control values of the diffusion coefficient were averaged and used for the rest of the optimization of the parameters except those at room temperature. The adjustable remaining parameters in the model were the transport coefficients K_1 and K_2.

Since there is no net efflux of total (tagged plus untagged) sodium ions from the cells at steady state, $K_1 \cdot C_{Na,e} = K_2 \cdot C_{Na,i}$. Thus, the ratio of K_1 to K_2 becomes equal to the concentration ratio, ϕ:

$$\frac{K_1}{K_2} = \frac{C_{Na,i}}{C_{Na,e}} = \phi \qquad (64)$$

Parameters K_1 and ϕ were optimized in this work. From the values of K_1 and ϕ, values of K_2, P_{Na}, S, $C_{Na,i}$, passive net influx, and passive efflux were calculated.

V. RESULTS AND DISCUSSION

Results

This work has mainly been confined to the evaluation of both the cell membrane permeability to sodium and the rate of active transport of sodium through the cell membrane in vascular smooth muscle in vitro. The effects of lowering extracellular potassium concentration and temperature on the membrane permeability and on the rate of active transport through the membrane were also investigated.

The Cell Membrane Permeability to Sodium

Figure 12 shows the results of a typical experiment to measure the Na^{22} effluxes from isolated segments of canine femoral artery in normal Ringer's at 37°C. As mentioned earlier, the loss of Na^{22} from the tissue occurred mainly in two stages--a fairly rapid diffusion of Na^{22} from the extracellular space, being followed by a relatively slow exchange of intracellular sodium. These two processes so closely interact with each other that it is impossible to resolve the washout curve into the two individual processes as has been attempted by others (21, 24, 39). Instead, a parameter optimization procedure using the KINFIT program (19) was employed to fit the entire washout curve to the model [Equations (50) and (51)].
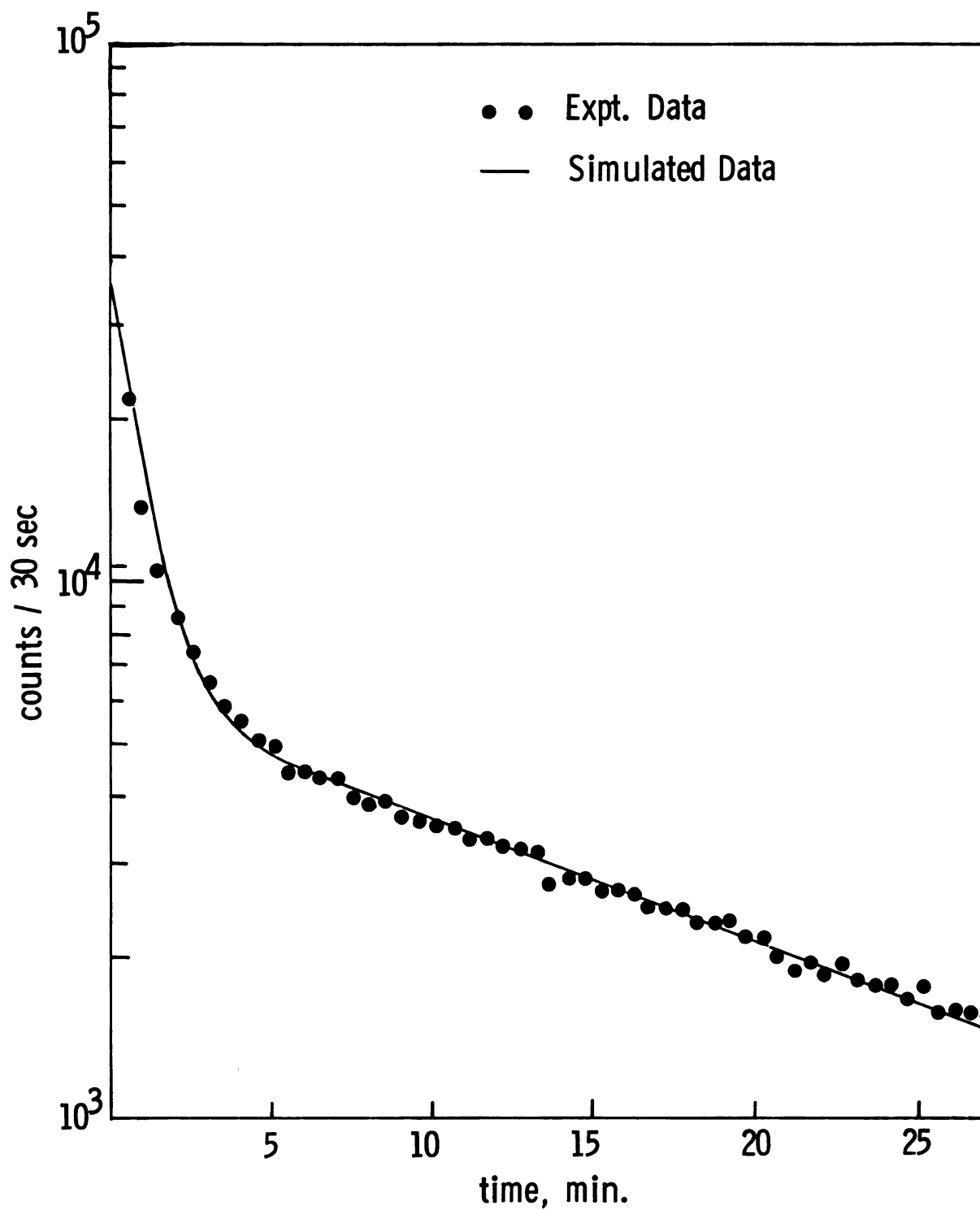
Figure 12.--Na^{22} efflux from arterial wall at 37°C. The tissue was both incubated and washed in normal Ringer's.

Twelve initial control experiments were performed and the results were analyzed based on the model. The optimized values of the parameters were obtained from each experiment and the mean value of each parameter with its standard deviation was calculated. Dimensions of the twelve tissues used for the experiment and the values of the initial differential count rates determined from the washout data are given in Table 2. The value of 8.33×10^{-6} cm^2/sec used for the diffusion coefficient was the mean value of the data on the diffusion coefficient obtained through the preliminary optimizing process for the twleve control runs. The twelve individual data are also given in Table 2. The values for the parameters are listed in Table 3 along with the values for other cellular properties calculated based on the parameters.

For comparison, Table 4 (page 80) gives the values of K_2 obtained by other investigators. The value of K_2 from this work is approximately twice that found by Jones and Karreman (33) based on the association-induction hypothesis and about a half of the values obtained from the graphical method.

It is now well accepted that the intracellular sodium concentration of vascular smooth muscle is higher than those in other types of muscles. The reported values range from 12 (32) to 50 mEq/l (21). The data on the intracellular sodium ion concentration show a wide variation mainly because of the uncertainties involved in quantifying the amount of bound ions and the size of the intracellular space. Since the intracellular concentrations obtained from this work account only for freely diffusible ions, they would

TABLE 2.--Dimensions of the tissues used for control experiments, their differential initial count rates and values of diffusion coefficients.

No.	Inside Radius cm	Outside Radius cm	Length cm	$N^*(0)$	$D \times 10^6$ cm^2/sec
1	0.0673	0.0990	1.7864	728	7.5
2	0.0673	0.1030	1.9480	755	9.5
3	0.0673	0.0986	1.8125	580	7.5
4	0.0673	0.0898	1.6897	447	7.7
5	0.065	0.1015	1.6715	1,140	7.8
6	0.065	0.0988	1.8640	1,840	9.0
7	0.065	0.0937	1.3132	775	7.5
8	0.065	0.0921	1.8077	1,086	9.3
9	0.065	0.1160	1.6506	2,214	8.3
10	0.065	0.0997	1.7001	975	9.0
11	0.065	0.0957	1.7276	1,560	8.8
12	0.065	0.1039	1.8363	1,940	8.0
Avg.					8.33
S.D.					0.73

TABLE 3.--Results of twelve control experiments at 37°C.*

No.	K_1 ($\times 10^8$) cm/sec	K_2 ($\times 10^8$) cm/sec	C_i/C_e	C_i mEq/l	P_{Na} ($\times 10^8$) cm/sec	S	Passive Efflux	Passive Influx
							mEq/cm^2 sec $\times 10^9$	
1	1.65	11.8	0.14	20.4	0.681	2.37	0.0398	2.41
2	1.60	11.3	0.14	20.7	0.661	2.3	0.0413	2.34
3	1.58	10.6	0.15	21.8	0.652	2.27	0.0407	2.31
4	1.42	14.6	0.10	14.2	0.586	2.05	0.0231	2.07
5	1.84	8.98	0.21	29.9	0.76	2.62	0.0651	2.69
6	0.93	12.85	0.07	10.6	0.384	1.35	0.0162	1.36
7	0.84	12.46	0.07	9.8	0.345	1.21	0.0097	1.22
8	1.64	8.54	0.19	28.0	0.677	2.34	0.0543	2.39
9	2.55	19.61	0.13	19.0	1.053	3.67	0.0572	3.72
10	1.15	8.71	0.13	19.3	0.475	1.65	0.0262	1.68
11	0.89	11.32	0.08	11.5	0.368	1.29	0.0108	1.30
12	1.39	10.69	0.13	19.0	0.574	2.00	0.0312	2.03
Avg.	1.45	11.80	0.128	18.7	0.601	2.09	0.0346	2.13
S.D.	0.48	3.0	0.044	6.4	0.2	0.685	0.0183	0.7

*K_1 = rate constant for influx

K_2 = rate constant for efflux

C_i = intracellular sodium concentration

C_e = extracellular sodium concentration

P_{Na} = membrane permeability to sodium ions

S = rate of active transport of sodium ions through the cell membrane

TABLE 4.—Value of $a \cdot K_2$.

Tissue	Animal	$a \cdot K_2$ (1/sec)	Method	Ref.
Carotid	Dog	2.31×10^{-3}	Graphical	21
Aorta	Rat	3.48×10^{-3}	Graphical	24
Carotid	Dog	0.5×10^{-3}	Ass.-Ind.	33
Femoral artery	Dog	1.18×10^{-3}	Diffusion	*

*This work.

be expected to be lower than other values estimated from the chemical analysis. The mean value of 18 mEq/l for the intracellular sodium concentration compares favorably with the value of 12 mEq/l found by Jones (32) with small arteries from the rat.

The calculated active and passive fluxes indicate that most of the efflux is due to active transport of the sodium ion. This is not unexpected since the driving forces for passive transport result in a large influx of sodium. The rate of active transport of sodium ions and the cell membrane permeability to sodium ions have never been evaluated in the past except for the values for the membrane permeability obtained based on a passive flux model only.

Effects of Lowering Extracellular Potassium Level on Na-Efflux

A decreased sodium efflux with lowered external potassium concentration has been reported for various types of muscle including smooth muscle (21, 24, 25, 35). The particularly high

potassium-dependency of Na-efflux is characteristic of vascular smooth muscle (21).

Experiments were performed at two lowered potassium levels: at one-half and at one-quarter of the normal 4.0 mEq/l. In order to maintain a chemical steady state throughout the experiment, the tissues were incubated for 120 minutes in Ringer's solution of the same composition as that to be used for washing the tissue. Typical washout data of two groups of experiments are shown in Figures 13 and 14, respectively. Listed in Table 5 (page 84) are the dimensions of the tissues used for the experiments and the initial differential count rates. The results of the experiments are given in Table 6 (page 85).

In order to compare the low potassium results with the control, hypothetical washout curves were generated using the average values for the parameters obtained from the control and low potassium experiments. They are normalized based on the initial count rates and shown in Figure 15 (page 86). On lowering the potassium level to 2 mEq/l, the washout rate of Na^{22} decreased. The mean value for the rate of active transport of sodium ions was also 13% less than the control value, but no statistical significance could be found for this change. There was no significant change in permeability (see Table 11, page 100).

By further reducing the extracellular potassium level down to 1.0 mEq/l the apparent rate of active transport was increased to about 50% greater than control, rather than being further decreased. Both the permeability and the intracellular sodium concentration
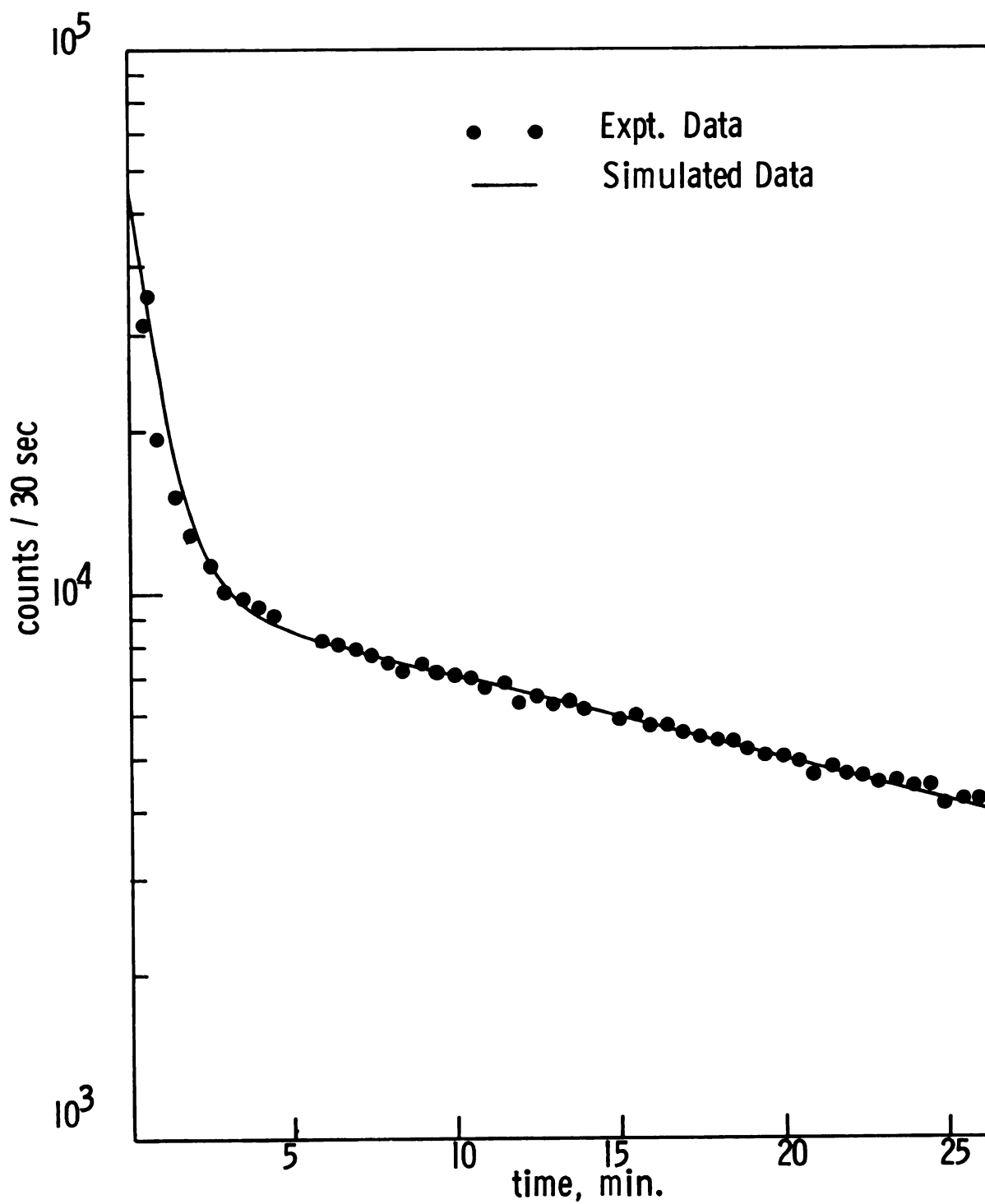
Figure 13.--Na^{22} efflux at 37°C. The tissue was both incu-
bated and washed in Ringer's with potassium concentration of
2 mEq/1.
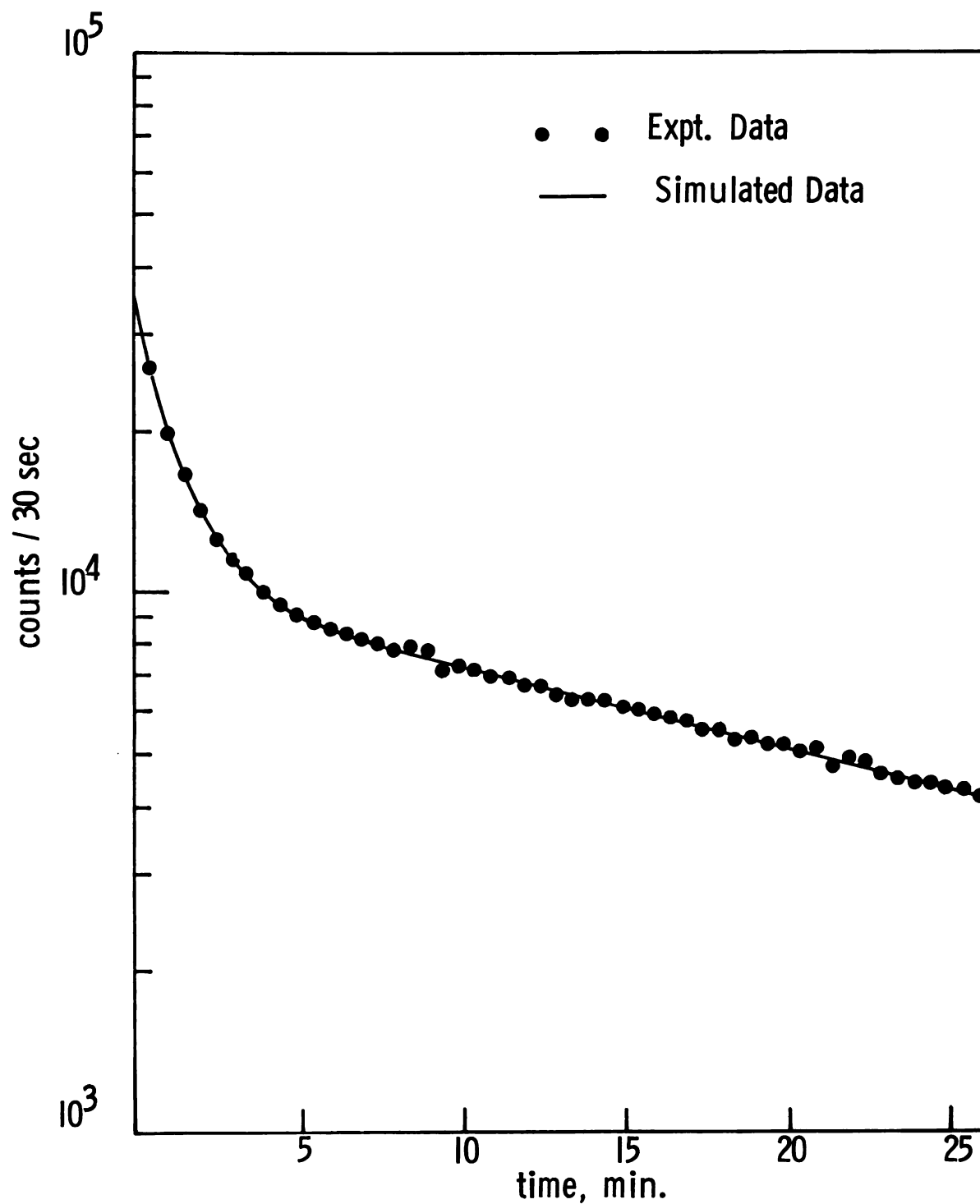
Figure 14.--Na^{22} efflux at 37°C. The tissue was both incu-
bated and washed in Ringer's with potassium concentration of
1 mEq/1.

TABLE 5.--Dimensions of the tissues used for washing experiments with Ringer's solution having potassium concentration of 2 mEq/l or 1 mEq/l and their differential initial count rates.

No.	Inside Radius cm	Outside Radius cm	Length cm	$N^*(0)$
1/2 [K$^+$]				
1	0.065	0.0989	1.6390	1,745
2	0.065	0.1033	1.8962	1,510
3	0.065	0.1059	1.7953	1,475
4	0.065	0.1018	1.8255	1,230
5	0.065	0.0906	1.6975	790
6	0.065	0.1033	1.8080	1,875
1/4 [K$^+$]				
1	0.065	0.1143	1.6083	1,155
2	0.065	0.1091	1.8488	1,136
3	0.065	0.0837	1.8193	420
4	0.065	0.1026	1.3833	1,030
5	0.065	0.1017	1.7338	1,650
6	0.065	0.1079	1.8345	2,430
7	0.065	0.0948	1.8568	970
8	0.065	0.1026	1.7319	2,140

TABLE 6.--Results of experiments with the tissues both incubated and washed in Ringer's solution with lowered potassium concentration at 37°C.*

No.	K_1 (x 10^8) cm/sec	K_2 (x 10^8) cm/sec	C_i/C_e	C_i mEq/l	P_{Na} (x 10^8) cm/sec	S	Passive Efflux mEq/cm^2 sec x 10^9	Passive Influx mEq/cm^2 sec x 10^9
1/2 K^+								
1	1.36	5.71	0.24	34.75	0.573	1.93	0.059	1.99
2	1.79	6.00	0.30	43.50	0.754	2.51	0.098	2.63
3	1.87	6.76	0.28	40.30	0.787	2.63	0.094	2.73
4	1.10	5.60	0.20	28.76	0.465	1.57	0.040	1.61
5	0.68	9.88	0.07	10.07	0.287	0.99	0.009	1.00
6	0.57	5.44	0.10	15.18	0.239	0.82	0.011	0.83
Avg.	1.23	6.57	0.197	28.76	0.518	1.74	0.0518	1.80
S.D.	0.546	1.690	0.093	13.56	0.230	0.759	0.0392	0.800
1/4 K^+								
1	2.20	5.41	0.41	59.28	1.129	2.92	0.029	3.21
2	2.52	5.97	0.42	61.76	1.298	3.34	0.034	3.68
3	1.41	7.30	0.19	28.18	0.725	1.97	0.009	2.06
4	3.80	8.15	0.47	68.04	1.955	4.98	0.047	5.55
5	1.94	13.59	0.14	20.88	1.000	2.75	0.009	2.84
6	2.97	11.34	0.26	38.25	1.529	4.09	0.025	4.34
7	2.42	17.44	0.14	20.29	1.247	3.43	0.011	3.54
Avg.	2.47	9.89	0.29	42.38	1.269	3.35	0.023	3.60
S.D.	0.764	4.436	0.139	20.36	0.380	0.971	0.0147	1.116

*K_1 = rate constant for influx
K_2 = rate constant for efflux
C_i = intracellular sodium concentration
C_e = extracellular sodium concentration
P_{Na} = membrane permeability to sodium ions
S = rate of active transport of sodium ion through the membrane
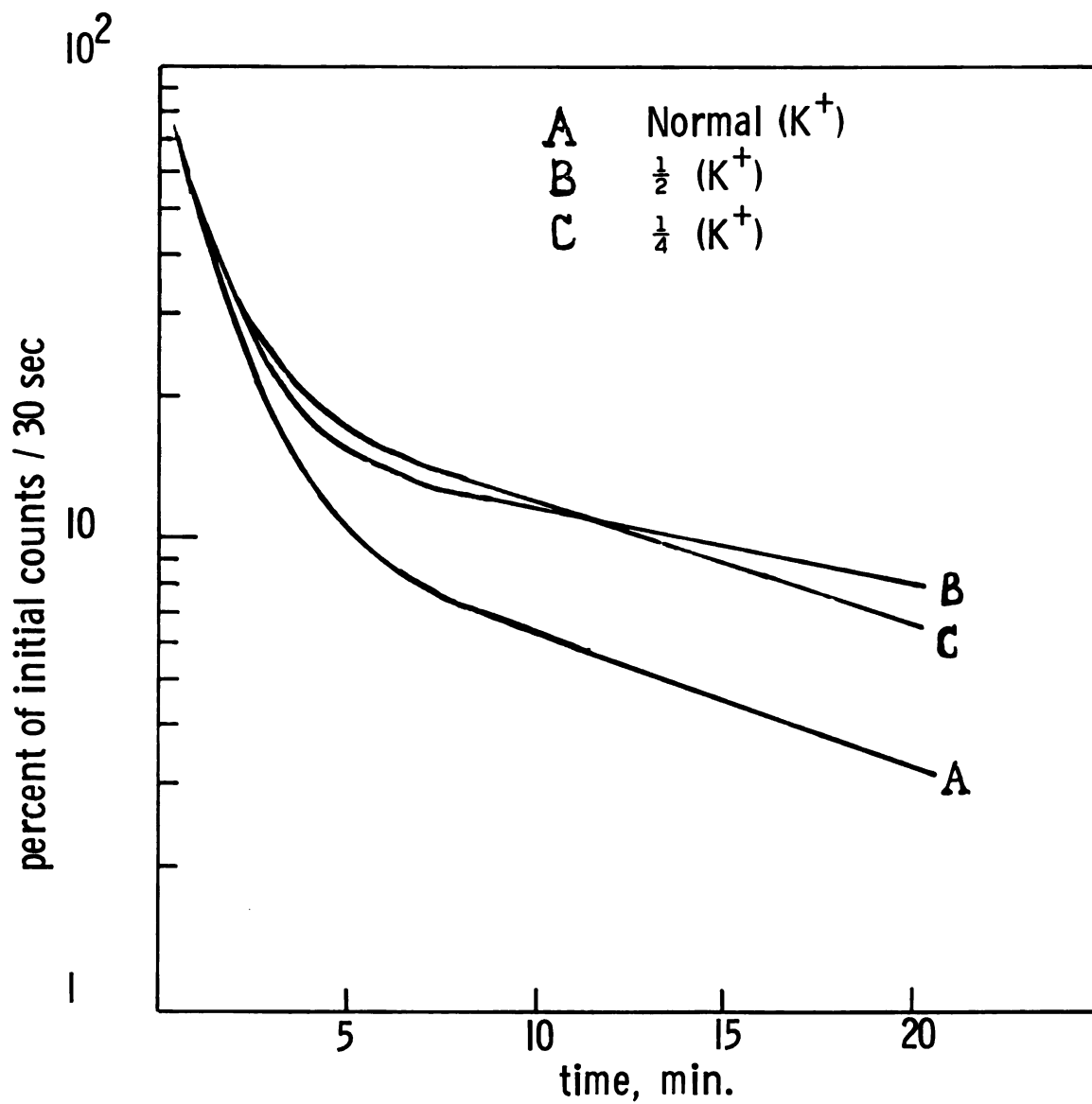
Figure 15.--Simulated washout curves (normalized based on the initial count rates) using the average values for the parameters.

were approximately double the normal values (see Table 11, page 100).
The increase in active transport is totally unexpected and may be
an indication of problems with the experimental technique at low
potassium concentration, etc.

Effects of Incubating Condition on Na-Efflux

With a sudden change in potassium composition of the bathing
solution, the tissue will go through a transient period until it
reaches a new steady state in the altered environment. During this
period it becomes difficult to analyze the washout data in terms of
a mathematical model unless the parameters in the model are known
as a function of time over the transient period.

In most previous washout studies on vascular smooth muscles,
the effect of changing potassium concentration has been investigated
by simply altering the potassium composition of the washing medium
and not the initial incubate, the results being analyzed as if the
tissues were in a steady state.

In order to maintain a constant chemical composition during
the wash period, Na^{22} incubating solutions were used with the same
concentrations as the washing solutions. The 120 minute incubation
period thus brought the cells to a new steady state chemically as
well as tagging the tissue with tracer. The wash period should,
therefore, be at steady state chemically.

For the washout experiments in which Ringer's solution with
potassium concentration of 1 mEq/l was used for washing the tissues,
tissues were incubated in Ringer's with potassium concentration of

4 mEq/l (normal) as well as in Ringer's with the same potassium

concentration as the washing solution (1 mEq/l) to see any effect

of incubating condition on sodium efflux. A typical washout curve

obtained with a tissue incubated in normal Ringer's is shown in

Figure 16 and its normalized curve is compared with that for the

tissue both incubated and washed in Ringer's with 1 mEq/l of potas-

sium in Figure 17.

The membrane potential, which is required for the analysis

of washout data, is expected to change during a transient period

due to changing the potassium composition in the washing solution.

Since no experimental data on those changes through the transient

period are available, calculated values based on a model were

used for the optimization of the parameters. Figure 18 shows pre-

dicted changes in resting membrane potential due to a step change

in the external potassium concentration from the normal 4 mEq/l to

1 mEq/l, using Brace's model (9). After the first five minutes the

rate of change becomes so slow that the membrane potential may be

assumed constant. A value of 46 mV based on this predication was

used for the analysis of the washout data.

Table 7 (page 92) shows the dimensions of tissues used for

experiments and the initial differential count rates. The optimized

values for the parameters and other values obtained from these

parameters are given in Table 8 (page 93).

There are significant differences in the values for the K_1,

P_{Na}, S, and $[Na^+]_i$ between the two experiments. Though the values

for the tissues incubated in normal Ringer's are of necessity based
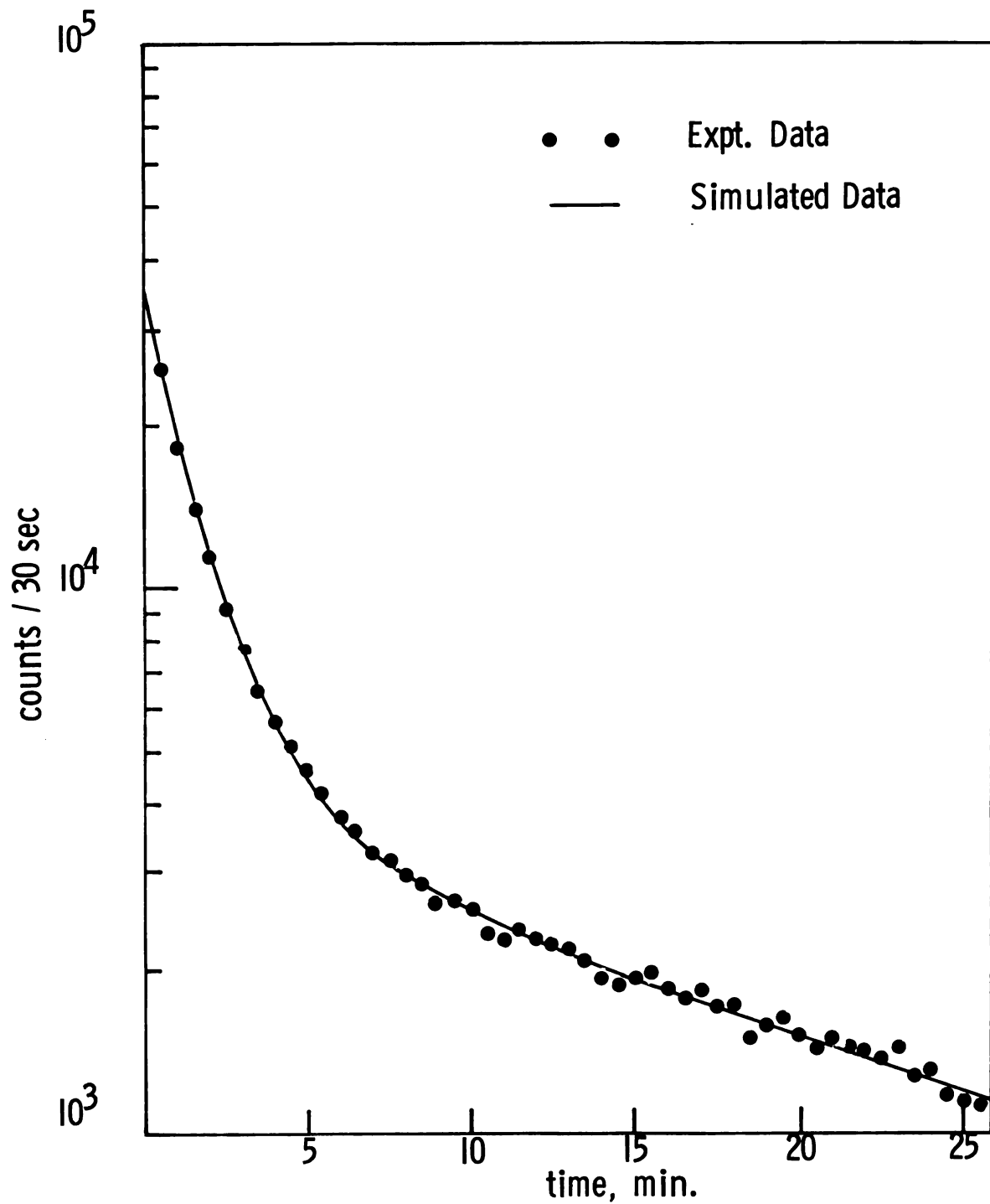
Figure 16.--Na^{22} efflux at 37°C. The tissue was incubated in normal Ringer's and washed with Ringer's having potassium concentration of 1 mEq/l.
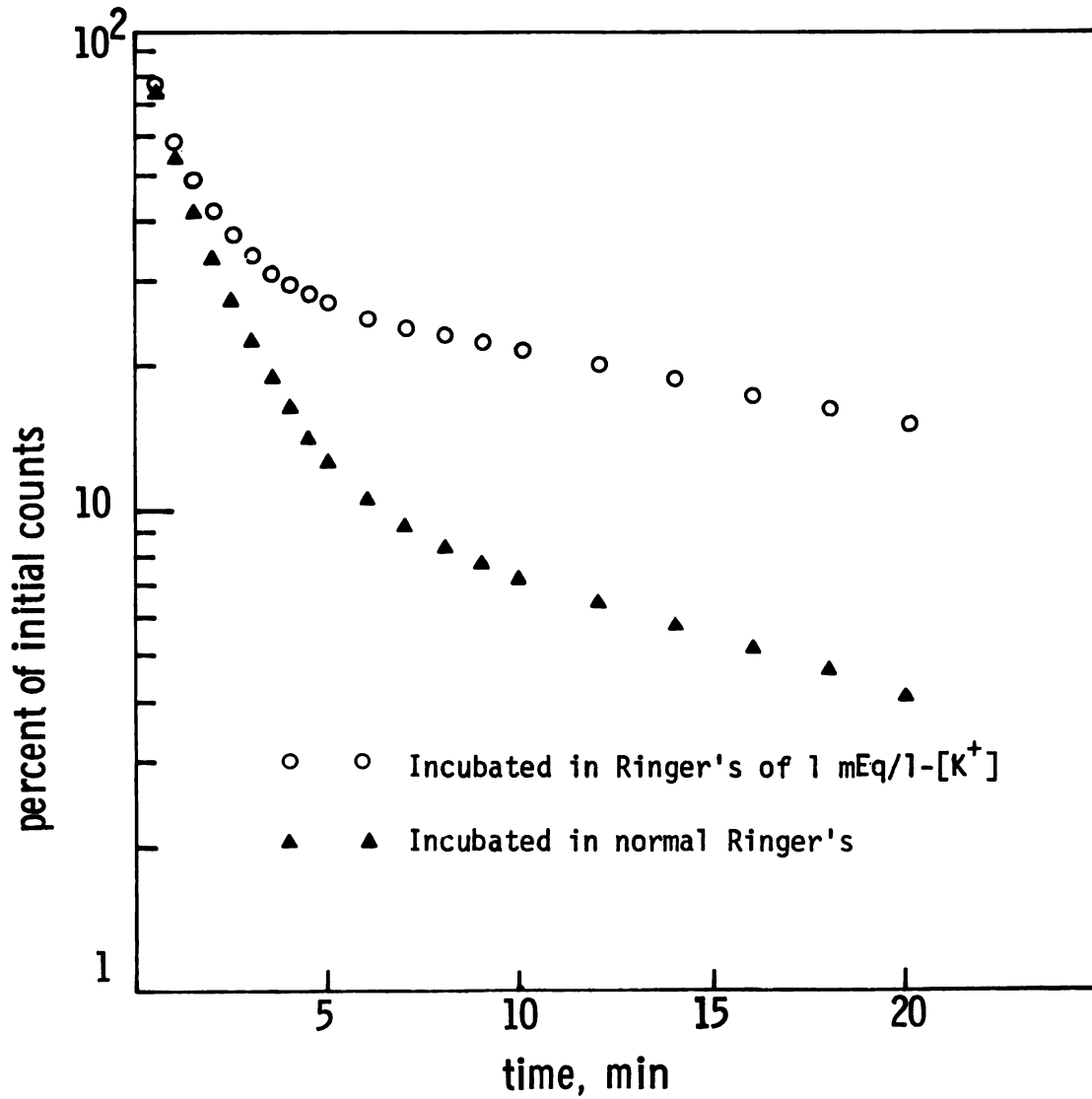
Figure 17.--Normalized washout curves obtained with tissues washed with Ringer's having 1 mEq/l of potassium after being incubated in normal Ringer's or in Ringer's of 1 mEq/l-[K$^+$].
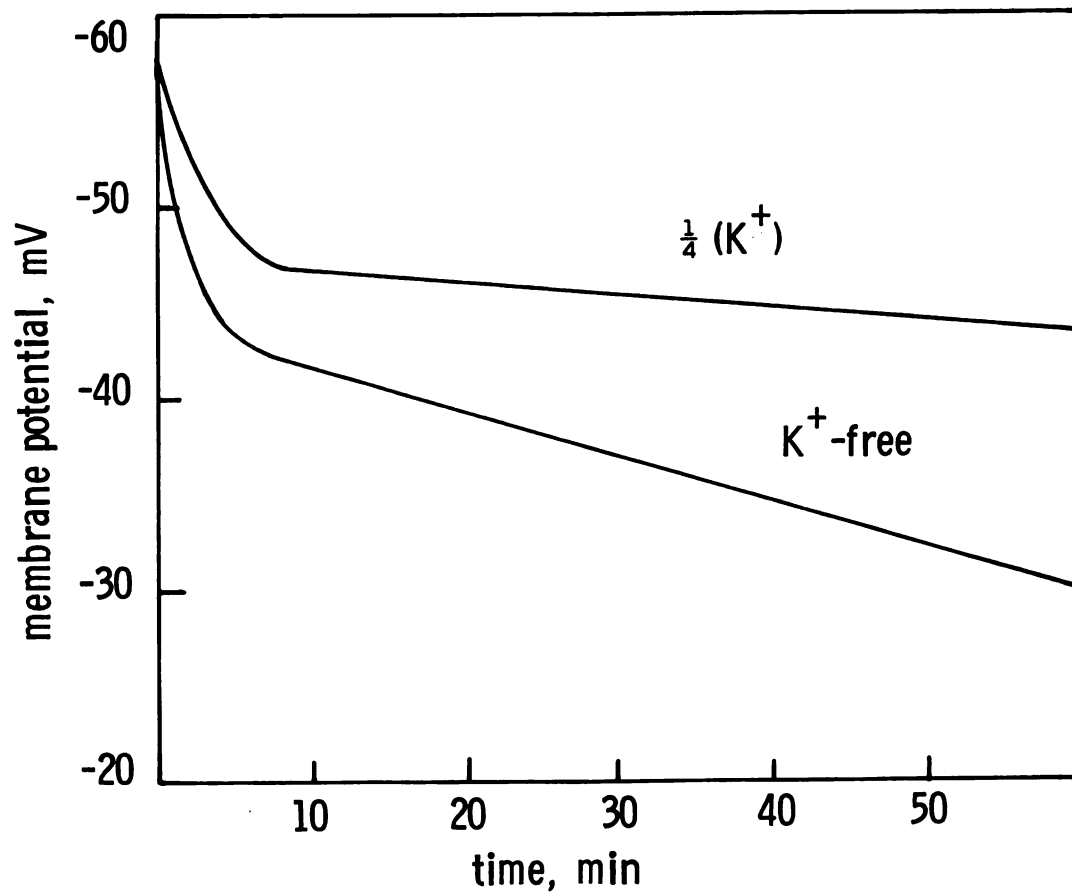
Figure 18.--Resting membrane potential as a function of time when the external potassium concentration changed to 1 mEq/l or zero.

TABLE 7.--Dimensions of the tissues used for experiments to observe the effect of incubating condition on sodium efflux.

| No.	Inside Radius cm	Outside Radius cm	Length cm	$N^*(0)$
1/4 $[K^+]$				
1	0.065	0.1100	1.8829	668
2	0.065	0.1032	1.5532	1,100
3	0.065	0.1001	1.8272	1,200
4	0.0673	0.1078	1.5168	1,328
5	0.065	0.0939	1.8719	750
6	0.065	0.1149	1.8748	1,170
$[K^+]$-free				
1	0.0673	0.0880	1.8004	568
2	0.0484	0.0852	1.5741	940
3	0.0484	0.0832	1.6549	610
4	0.0484	0.0810	1.6965	815
5	0.0484	0.0830	1.6747	519
6	0.0484	0.0808	1.7109	554
7	0.0484	0.0910	1.7117	620
8	0.0484	0.0909	1.8520	790
9	0.0484	0.0868	1.8056	960

TABLE 8.--Results of experiments with tissues incubated in normal
Ringer's solution and washed with low potassium or
potassium-free Ringer's solution at 37°C.*

No.	K_1 (x 10^8) cm/sec	K_2 (x 10^8) cm/sec	C_i/C_e	C_i mEq/l	P_{Na} (x 10^8) cm/sec	S	Passive Efflux	Passive Influx
							mEq/cm^2 sec x 10^9	
1/4 K^+								
1	1.23	7.43	0.17	24.24	0.588	1.75	0.0220	1.80
2	0.98	10.08	0.10	14.16	0.466	1.40	0.0174	1.43
3	0.75	9.24	0.08	11.83	0.357	1.08	0.0137	1.09
4	0.41	7.66	0.05	7.74	0.194	0.59	0.0073	0.59
5	1.92	10.59	0.18	26.43	0.913	2.71	0.0342	2.80
6	1.03	8.51	0.12	17.67	0.491	1.47	0.0184	1.50
Avg.	1.05	8.92	0.12	17.01	0.502	1.50	0.0188	1.54
S.D.	0.509	1.278	0.050	7.242	0.242	0.713	0.0090	0.743
K^+-free*								
1	1.38	8.45	0.16	23.80	0.724	1.93	0.0320	2.01
2	0.26	6.36	0.04	5.97	0.137	0.38	0.0060	0.38
3	0.49	10.08	0.05	7.15	0.260	0.71	0.0148	0.72
4	1.17	10.94	0.11	15.62	0.615	1.67	0.0271	1.71
5	1.84	7.74	0.24	34.75	0.969	2.54	0.0428	2.69
6	0.94	9.62	0.10	14.31	0.496	1.35	0.0219	1.38
7	1.78	8.48	0.21	30.66	0.936	2.47	0.0413	2.60
8	0.87	5.67	0.15	22.48	0.459	1.23	0.0203	1.27
9	0.74	8.66	0.09	12.41	0.387	1.05	0.0171	1.08
Avg.	1.05	8.44	0.13	18.57	0.554	1.48	0.0248	1.54
S.D.	0.543	1.691	0.0687	10.028	0.285	0.744	0.0122	0.793

*A value of 39 mV for the membrane potential was used for the
analysis of K^+-free washout data (based on Figure 18).

on an approximate analysis, it seems likely that the two experiments do indeed lead to different results. Compared with the results of the experiments with tissues incubated in Ringer's with potassium concentration of 1 mEq/l, the rate of active transport, permeability, and the intracellular sodium concentration were reduced by approximately 50%. Only the value of K_2 was about the same (see Table 11, page 100).

Similar experiments were performed using K-free Ringer's, namely, the tissues were incubated in normal Ringer's and washed with potassium-free Ringer's. The calculated resting membrane potentials in K-free Ringer's were again obtained using Brace's model (9) and are shown in Figure 18 (page 91). The change in potential continued to drop over the washout period, not allowing a steady state approximation. The washout data, however, were also analyzed based on the model because no other method was available. The results are given in Table 8 (page 93). Table 7 (page 92) also includes the dimensions of the tissues used for these experiments and their initial differential count rates. In general, the results of the experiments with tissues incubated in normal Ringer's and washed with K-free Ringer's are not much different from those of experiments with tissues incubated in normal Ringer's and washed with Ringer's having potassium concentration of 1 mEq/l. Figure 19 shows a typical washout curve of these experiments.
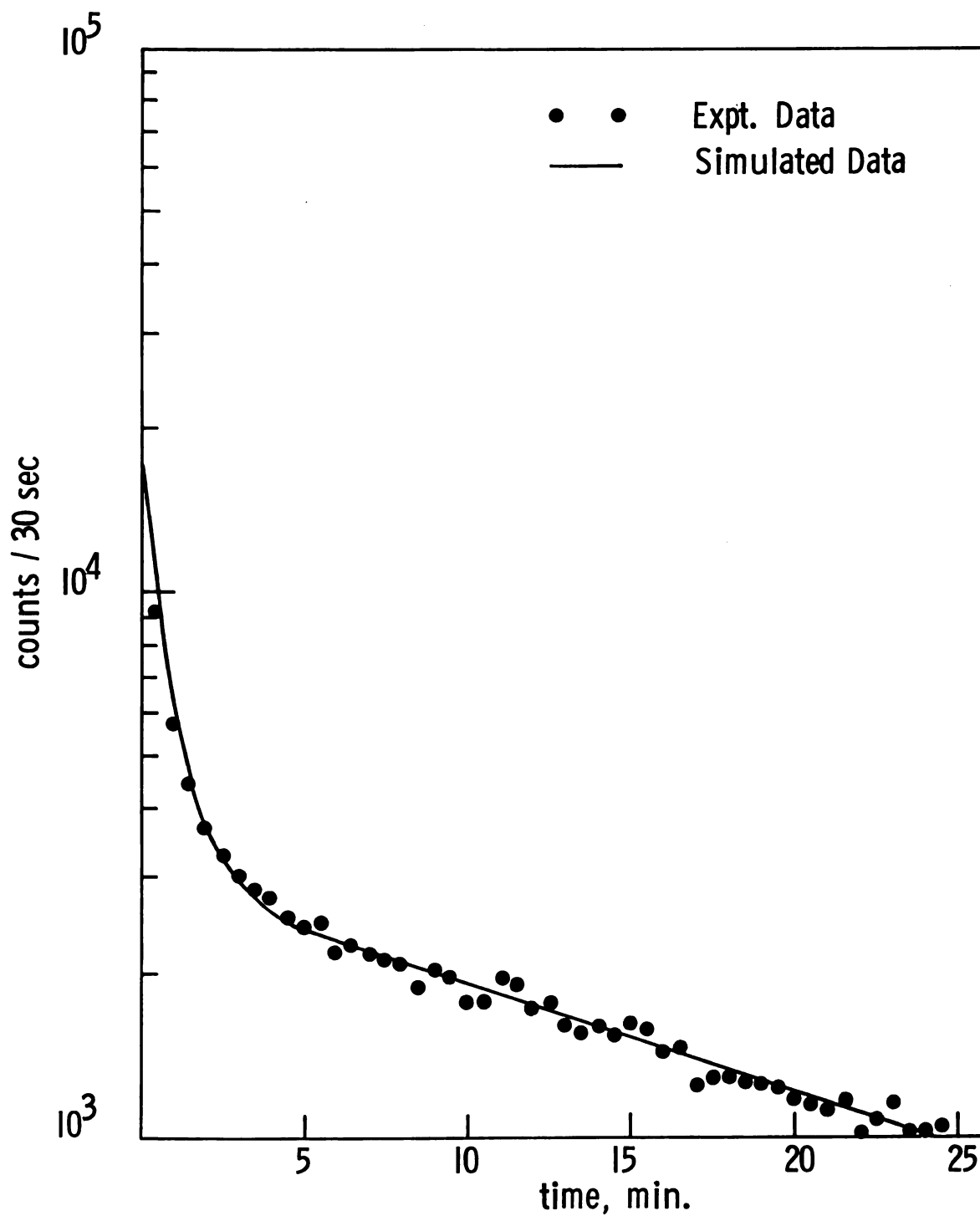
Figure 19.--Na^{22} efflux at 37°C. The tissue was incubated in normal Ringer's and washed with K$^+$-free Ringer's.

Temperature Effects on Na-Efflux

In order to observe temperature effects on sodium efflux, experiments were performed at two different temperature levels, 37°C and room temperature (21 ± 2°C).

Four experiments were performed at room temperature and the optimized values for the parameters and other calculated data based on the parameters are given in Table 10. Dimensions of the tissues used for experiments and the differential initial count rates are listed in Table 9 along with the values for diffusion coefficient obtained through the optimization process. A typical washout curve is shown in Figure 20 and its normalized curve is compared with that for the control experiment in Figure 21.

Finally, all the average values of the parameters and the other membrane properties from this work are summarized in Table 11 for comparison.

Discussion

In view of the relationship between changes in the cell potential and the contractile process of vascular smooth muscle, it appears that any factor which affects the membrane potential (either ionic composition, membrane permeability, active ionic flux, or any combination of these) may play a very important role in contraction.

In order to elucidate the roles of ions in muscle action, the exchange of sodium ions between the muscle cells and surrounding media has been studied by many investigators (17, 21, 24, 27). In

TABLE 9.--Dimensions of the tissues used for experiments at room
temperature (21 ± 2°C), their differential initial count
rates and values of diffusion coefficients.

No.	Inside Radius cm	Outside Radius cm	Length cm	$N^*(0)$	$D \times 10^6$ cm^2/sec
1	0.065	0.1150	1.4920	788	7.0
2	0.065	0.1211	1.8550	842	7.5
3	0.065	0.1050	2.0581	750	6.5
4	0.065	0.0950	1.4866	1,490	6.5
Avg.					6.88

TABLE 10.--Results of experiments at room temperature (21 ± 2°C).*

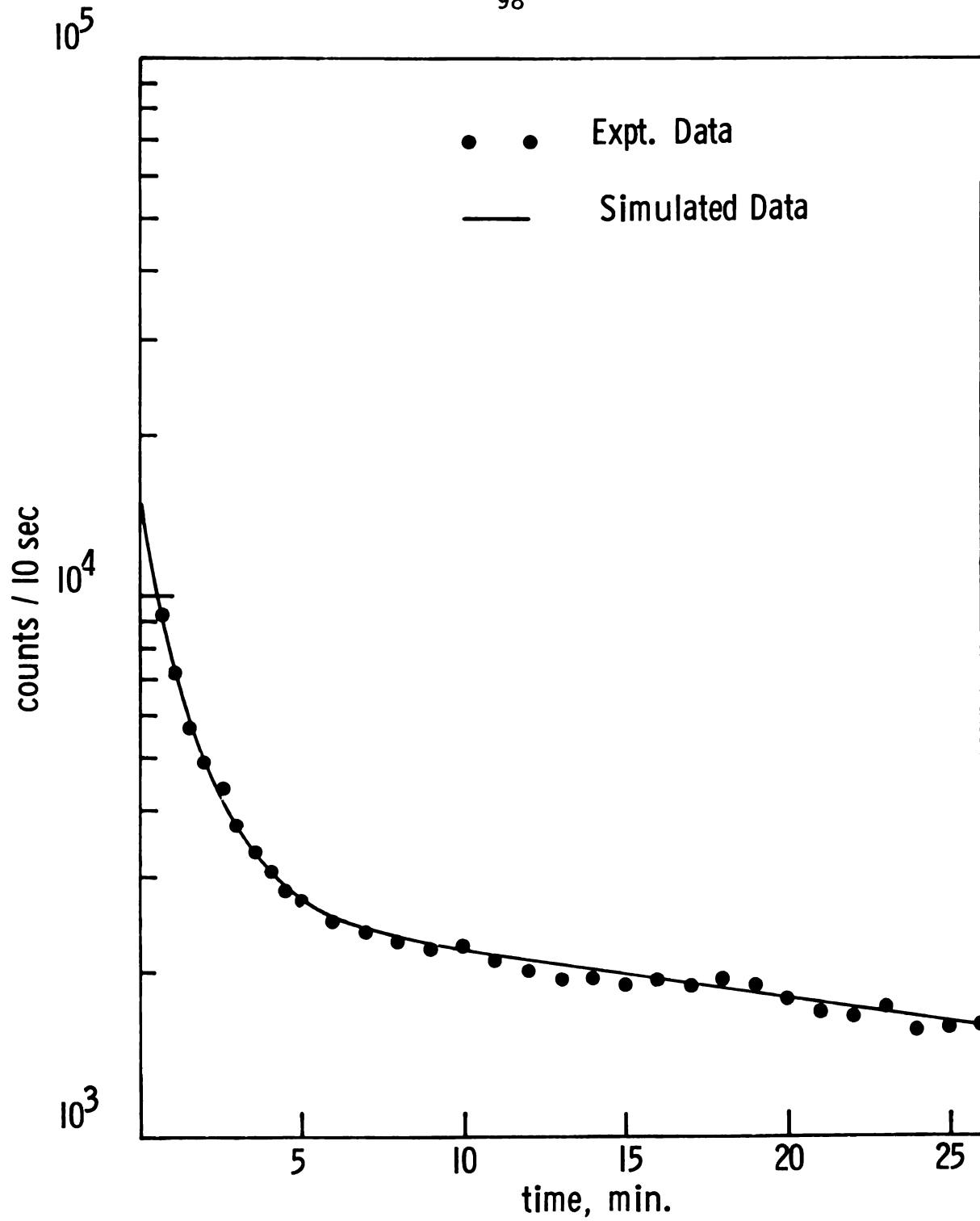| No.	K_1 $(\times 10^8)$ cm/sec	K_2 $(\times 10^8)$ cm/sec	C_i/C_e	C_i mEq/l	P_{Na} $(\times 10^8)$ cm/sec	S	Passive Efflux mEq/cm² sec $\times 10^9$	Passive Influx
1	1.15	6.42	0.179	26.1	0.553	1.63	0.050	1.68
2	1.23	7.07	0.174	25.4	0.591	1.75	0.052	1.80
3	1.10	6.47	0.17	24.8	0.529	1.55	0.045	1.60
4	0.82	3.57	0.23	33.6	0.394	1.15	0.045	1.20
Avg.	1.08	5.9	0.19	27.5	0.520	1.52	0.048	1.57
S.D.	0.18	1.57	0.028	4.12	0.086	0.26	0.0036	0.26

Figure 20.--Na^{22} efflux at room temperature (21 ± 2°C).
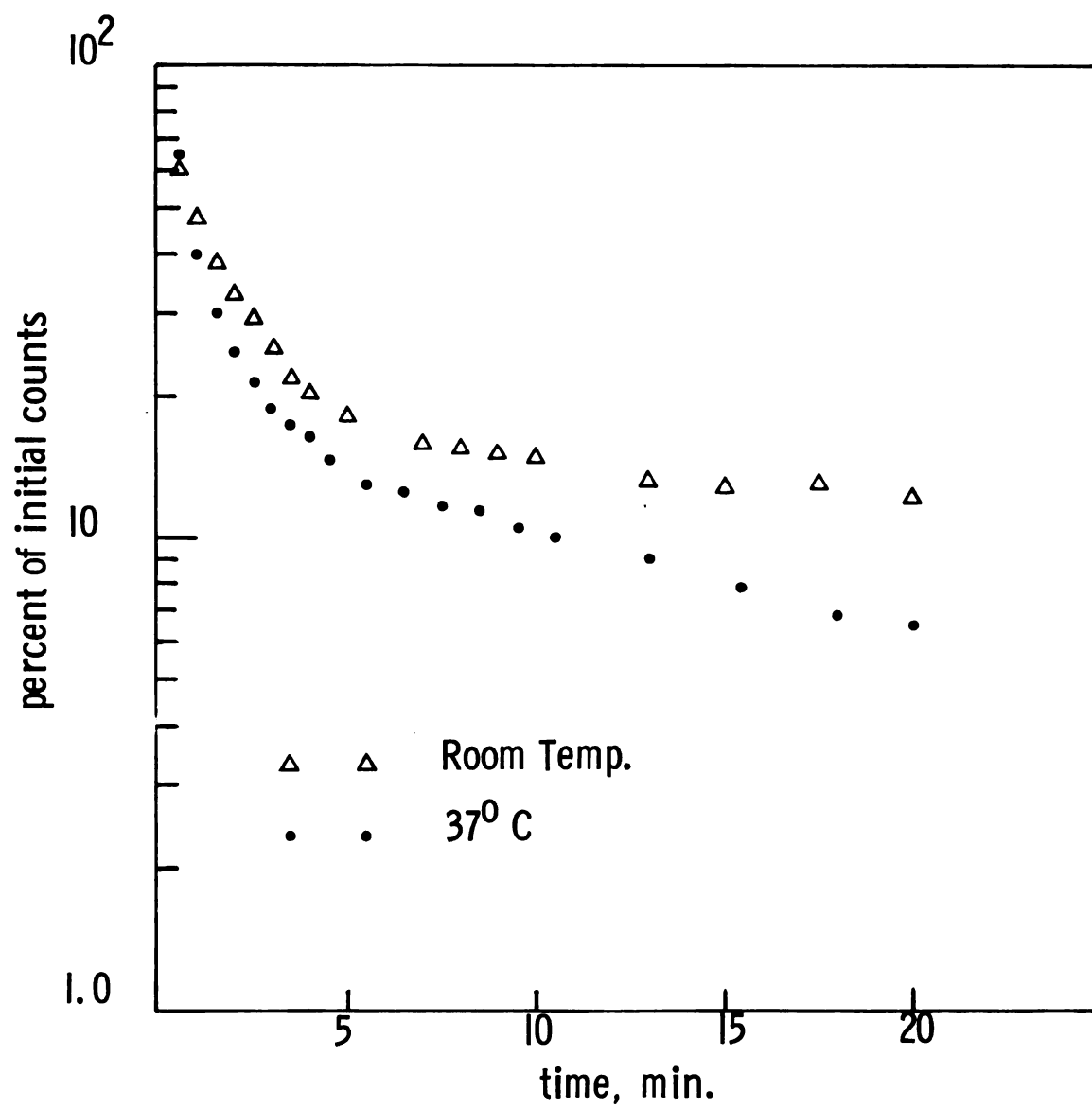The tissue was both incubated and washed in normal Ringer's.

Figure 21.--Comparison of the normalized washout curves
obtained with tissues both incubated and washed in normal Ringer's
at 37°C and room temperature, respectively.

TABLE 11.--Summary of the results.

Experiment Conditions	K_1 ($\times 10^8$) cm/sec	K_2 ($\times 10^8$) cm/sec	c_i/c_e	c_i mEq/l	P_{Na} ($\times 10^8$) cm/sec	S ($\times 10^9$) mEq/cm^2 sec
Control Temp 37°C Em = 57 mV	1.45 (±0.48)	11.80 (±3.0)	0.13 (±0.044)	18.7 (±6.4)	0.601 (±0.2)	2.09 (±0.685)
Temp effect Temp = 21 2°C Em = 57 mV	1.08 (±0.18)	5.9 (±1.57)	0.19 (±0.028)	27.5 (±4.12)	0.520 (±0.0857)	1.52 (±0.26)
Effect of lowering [K+]e Em = 55.4 mV [K+]e = 2 mEq/l	1.23 (±0.546)	6.57 (±1.69)	0.20 (±0.093)	28.76 (±13.565)	0.518 (±0.23)	1.74 (±0.579)
Effect of lowering [K+]e Em = 40.5 mV [K+]e = 1 mEq/l	2.47 (±0.764)	9.89 (±4.436)	0.29 (±0.139)	42.38 (±17.01)	1.269 (±0.38)	3.35 (±0.971)
Effect of incubating condition* Em = 46 mV [K+]e = 1 mEq/l	1.05 (±0.509)	8.92 (±1.278)	0.12 (±0.0496)	17.01 (±7.242)	0.502 (±0.2423)	1.50 (±0.713)
Washing with K+-free Ringer's** Em = 39 mV	1.05 (±0.543)	8.44 (±1.691)	0.13 (±0.0687)	18.57 (±10.03)	0.554 (±0.285)	1.48 (±0.744)

*Incubated in normal Ringer's and washed with Ringer's of 1 mEq/l-[K+].
**Incubated in normal Ringer's and washed with K+-free Ringer's.

those studies, the washout curves have usually been fitted to a sum of exponentials, based on compartmental analysis. The washout data are then interpreted in terms of the exponential factors obtained from the washout curve using graphical methods. In general, more than two exponentials are required to fit the washout curve, suggesting that tissues being studied consisted of at least three compartments (21, 24, 39). With the present anatomical knowledge, biological identification of the compartments which are implied in the analysis of the washout data offers a considerable problem. Also, the exponential factors obtained from the graphical peeling technique are not rate constants but, in fact, have a more complicated interpretation.

An approach similar to the one used here was taken by other investigators for the analysis of washout data. Harris and Burn (25) used essentially the same model for the study of ionic fluxes in frog satorius muscle but the data were analyzed by an approximate graphical technique and active pumping was not considered. Jones and Karreman (33) used a numerical technique with a computer to analyze the equivalent of Equations (50) and (51) and presented data for the exchange of sodium ions in canine carotid arteries. Based on a concept quite different from the compartmental model, they optimized the diffusion coefficient in the extracellular space. However, the values of the rate constants, K_1 and K_2, were obtained with the graphical method, which is based on the compartmental model. Thus none of the previous investigators have used a model which (a) considered diffusion in the extracellular space,

(b) interpreted the membrane transfer coefficients in terms of both passive and active fluxes, and (c) used computer optimization techniques to fit the data to the model. As a result, the methods presented here appear to be a significant improvement in the interpretation of tissue washout data.

Data at Normal Temperature and Potassium Concentration

Because of these considerations, we have used a model in this work to take into account diffusion in the extracellular space and to evaluate the rate constants, K_1 and K_2, for membrane transport using a digital computer. Some values of K_2 from other investigators are shown in Table 4 along with the value from this work, though such a comparison does not have much meaning because of the difference in the interpretations of the rate constant between investigators. The value from this work (11.8×10^{-8} cm/sec) is about a half of the values obtained with the graphical method and approximately twice that found by Jones and Karreman (33).

The rate constant, which is a lumped parameter, is a function of several membrane properties affecting ionic fluxes, including membrane potential, membrane permeability, rate of active transport, etc. Based on Goldman's constant field assumption, these properties were calculated from the data obtained in this study. Thus, we gained not only values for these parameters, but hopefully, a little deeper insight into the contractile mechanism.

The mean values for the diffusion coefficient of Na^+ (8.33×10^{-6} and 6.9×10^{-6} cm^2/sec at 37°C and room temperature,

respectively) compare favorably with the value of 7×10^{-6} found by Jones and Karreman (33) at 37°C and with the value of 1.247×10^{-5} cm^2/sec in aqueous solution at 25°C (44). The comparison with the latter value is not unreasonable since a correction factor in the order of 0.5 is to be expected for the tortuosity of the diffusion pass in the extracellular space. The agreement with Jones and Karreman is also encouraging since, as stated earlier, they used essentially the same mathematical model and computer assisted optimizing techniques to determine D (but not K_1 and K_2). For comparison, an alternate method for determining D was tried in this work with the use of Equation (26).

$$\frac{\bar{N}^*(t)}{t} = N^*(0) - N_e^*(0) \cdot \left[\frac{b^2}{b^2 - a^2}\right] \cdot \left[\frac{8}{3}\left(\frac{D}{\pi b^2}\right)^{1/2} \cdot t^{1/2} - \frac{D}{2b^2} \cdot t\right.$$

$$\left. - \left[\frac{2}{15}\right]\left[\frac{D^3}{\pi b^6}\right] \cdot t^{3/2} + \cdots \right] \tag{26}$$

The diffusion coefficient can be evaluated from the limiting slope of a plot of $\bar{N}^*(t)/t$ vs $\sqrt{t}$ (see Figure 10). However this method is very sensitive to the value of the intercept $N^*(0)$ (which is also determined from the same plot). The average value of D for the twelve control experiments using this approach was 10.13×10^{-6} cm^2/sec. Though this is not in excellent agreement with the optimized D (8.33×10^{-6}), it is close enough to give confidence in the value for $N^*(0)$ that was used in the optimization.

Jones (32) reported a value of 1.5 x 10^{-8} cm/sec for the membrane sodium permeability of rat aorta, which is about twice the value of 0.6 x 10^{-8} obtained from here. However, since his value was calculated based on the Goldman equation (23) involving only passive fluxes and did not account for extracellular diffusion, good agreement between the two values is not expected. In a simulation of Hendrickx and Casteels' (27) experimental data on the resting membrane potential of the rabbit's ear artery using the Brace model (9), Briggs (11) found a value of $P_{Na} = 0.6$ x 10^{-8} cm for the membrane permeability. The agreement of that calculated result with the one from this work lends credence to these results.

Since it has been shown that various types of cells, including smooth muscle cells, have active fluxes of ions across the cell membranes (Na-K pump) and probably all Na-K pumps are electrogenic (55), the error introduced by neglecting the electrogenic Na-K pump has become obvious, particularly in smooth muscle cells where the pump makes a considerable contribution to resting membrane potential.

The variation of reported values for the intracellular sodium concentration over a wide range (12 to 50 mEq/l) reflects difficulties involved in obtaining the cellular sodium concentration. As mentioned earlier, because of the complexity of the arterial wall structure, obtaining an exact value of the intracellular ion concentration is beyond our ability at present. Since only diffusible ions (not bound) are accounted in this work, the intracellular sodium concentration (18 mEq/l) is expected to be

lower than other values estimated from the chemical analysis. This value compares favorably with the value of 12 mEq/l found by Jones (32).

In any case, the exact values for the parameters depend on the choices of ε's, $\underline{a}$, and E_m, which are uncertain. Though the most agreeable values available in the literature were chosen for the parameters, there is still no agreement on those values.

Effects of Lowering Temperature

Because of the lack of experimental data at this time, values of P, S, etc., at low temperature and $[K^+]$ were calculated using predicted or assumed values of ε's, E_m, etc. If and when experimental values become available, the calculated permeabilities and fluxes must be reinterpreted. As a means of qualitative comparison, however, the results presented here are valuable.

The rate of Na^{22} efflux was reduced by lowering the temperature to 21°C. The dependency of diffusion processes on temperature explains the decreases in the values of D and K_1 at low temperature (see Table 11). The rate of active transport of sodium ions (S) was also reduced with the decrease in the temperature.

On the other hand, the intracellular sodium concentration was increased by about 50% of the control value. Many ion flux studies on isolated vascular smooth muscle (21, 24, 33) have shown that sodium efflux is reduced by lowering temperature. In fact, many investigators use reduced temperature (4°C) as a means of loading cells with Na^+. It is now generally believed that the

ouabain sensitive Na-K ATPase is intimately related to the pumping

mechanism. By lowering the temperature, the activity of the enzyme

is reduced and this reduced activity should be reflected as a

corresponding decrease in the rate of active transport. The reduced

rate of active transport is, then, expected to increase $[Na^+]_i$.

Thus, the results of this work for low temperature substantiate the

current understanding of the behavior of the Na-K pump.

Effects of Lowering Potassium Concentration

For the tissues both incubated and washed in Ringer's with

the lowered potassium concentrations, the intracellular sodium con-

centration was increased as the $[K^+]_e$ decreased (see Figure 22).

Based on the Na-K pump hypothesis, the activity of Na-K ATPase would

decrease with $[K^+]_e$, lowering the Na-K pumping rate. As with

cooling this lowered pumping rate would then result in the increase

in $[Na^+]_i$. However, with the tissues incubated in normal Ringer's,

the effect of lowering $[K^+]_e$ could not be observed. Even with

K^+-free Ringer's $[Na^+]_i$ remained almost constant as shown in

Figure 22. By washing the tissue incubated in normal Ringer's with

Ringer's having low potassium, an unsteady state will be provided,

causing uncertainties in the interpretation of the results. How-

ever, in this situation, it might be expected that some value between

the control and that for the tissue both incubated and washed in

Ringer's with low potassium will be obtained. But this was not the

case with the intracellular sodium concentration, which turned out

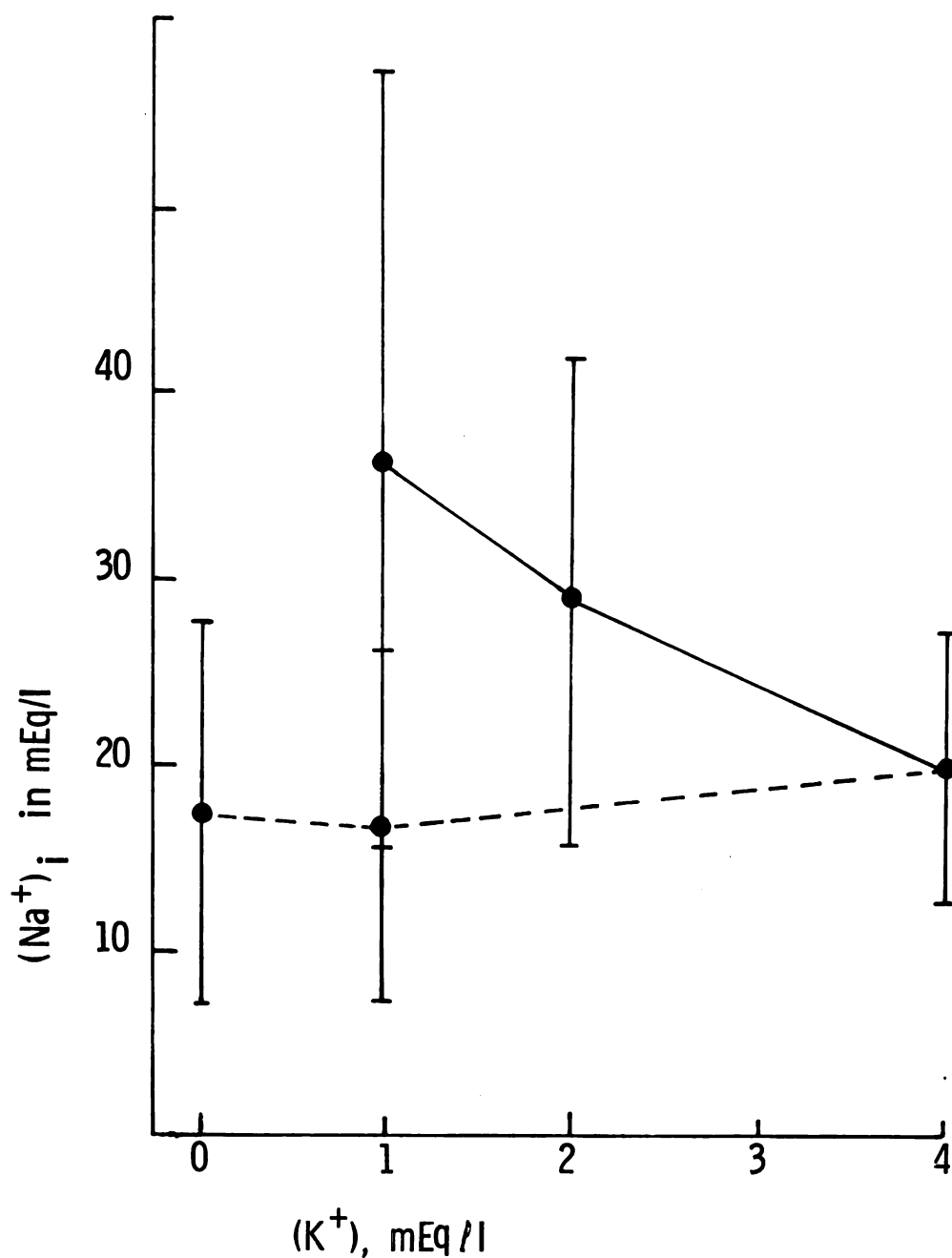to be almost the same as the control value. Perhaps when the tissue

Figure 22.--Intracellular sodium concentration as a function of external potassium concentration at 37°C. ●——●, data taken with tissues both incubated and washed in Ringer's with potassium concentration of 2 or 1 mEq/l. ●---●, data taken with tissues incubated in normal Ringer's and washed with Ringer's having 1 mEq/l of potassium or no potassium.

is incubated in normal Ringer's there is a continuous supply of potassium by the cells to provide a sufficiently high perimembrane potassium concentration for the normal activity of the Na-K pump even in lowered potassium or potassium-free Ringer's.

There were no statistically significant changes in the membrane permeability as the $[K^+]_e$ decreased, except when tissues were both incubated and washed in Ringer's with potassium concentration of 1.0 mEq/l as shown in Figure 23.

For the tissues both incubated and washed in Ringer's with 1.0 mEq/l of potassium concentration, the membrane permeability and the rate of active transport of sodium ions were increased (by 100% and 50% of control values, respectively). These results are unexpected because according to the Na-K pump hypothesis, the rate of active transport of sodium ions would decrease as the $[K^+]_e$ is reduced. These unexpected results may be due to inadequacy of the experimental technique. However, assuming the results are correct, one explanation might be that a severe increase in the intracellular sodium concentration, possibly due to the increase in the membrane permeability to sodium ions, stimulated the pump. The electrogenic nature of the pump might make this possible, even under lowered extracellular potassium level, through a change in the coupling ratio of the pump. From this consideration, one might speculate that a strong contraction of vascular smooth muscle may increase the membrane permeability.

As shown in Figure 24, there was a slight decrease in the mean rate of active transport (with the exception mentioned above)
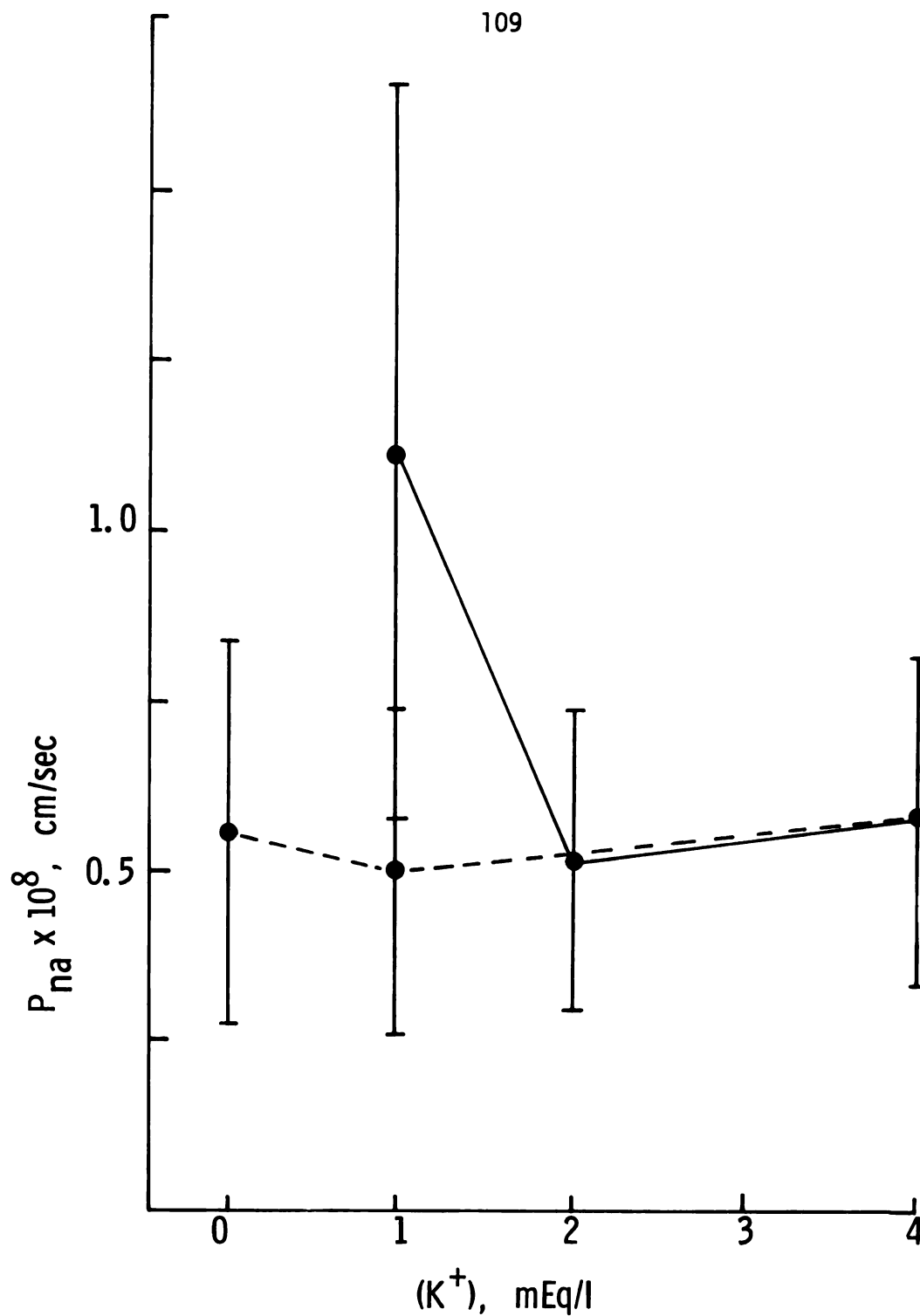
Figure 23.--Membrane sodium permeability as a function of external potassium concentration at 37°C. ●——●, data taken with tissues both incubated and washed in Ringer's with potassium concentration of 2 or 1 mEq/l. ●---●, data taken with tissues incubated in normal Ringer's and washed with Ringer's having 1 mEq/l of potassium or no potassium.
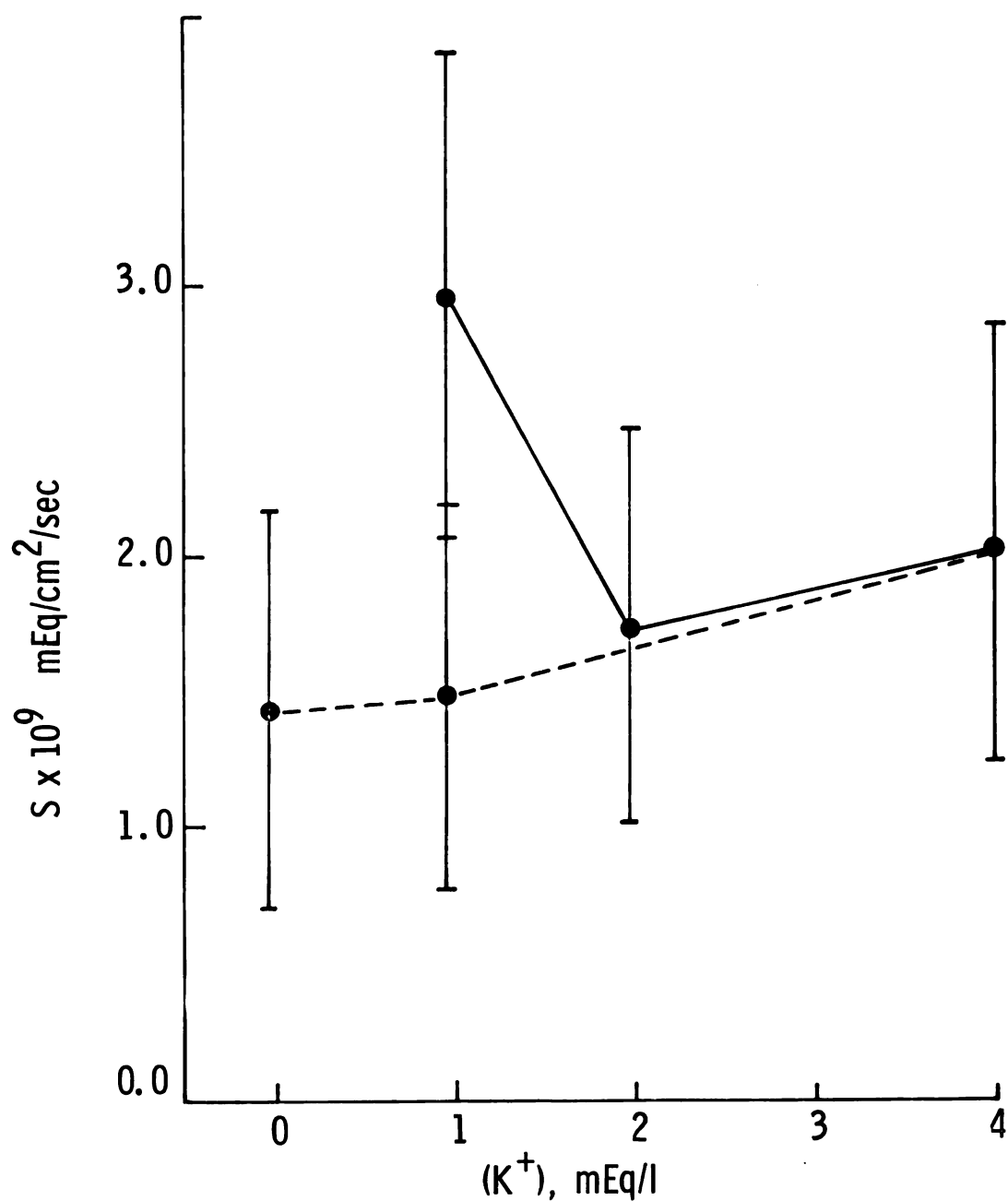
Figure 24.--Rate of active transport of sodium ions as a function of external potassium concentration at 37°C. ●——●, data taken with tissues both incubated and washed in Ringer's with potassium concentration of 2 or 1 mEq/1. ●---●, data taken with tissues incubated in normal Ringer's and washed with Ringer's having 1 mEq/1 or no potassium.

with lowered $[K^+]_e$, though no statistical significance could be given to the changes. These changes along with those of the intracellular sodium concentration are consistent with the Na-K pump hypothesis.

VI. CONCLUSIONS

From the results obtained from this study, the following conclusions may be made:

(a) In studies of mass transfer in blood vessel walls, diffusion in the extracellular space must be accounted for if one is going to attach physical significance to the parameters of the model.

(b) When studying the effect of varying ionic composition on mass transfer in tissue, the tissue should be incubated and washed in solutions of the same concentration.

(c) The findings of this study are consistent with the Na^+-K^+ pump theory for active transport.

(d) These studies have provided valuable information about the rate of active transport of sodium as well as the membrane permeability of vascular smooth muscle to sodium ions.

VII. RECOMMENDATIONS

All of the calculated results of this work were obtained using a set of assumed values for ε_i, ε_e, and E_m. They were based on literature data for selected tissues. An attempt was made in this work to maintain tension in the tissue during the experiments. From the results, particularly for the case where the tissues were both incubated and washed in Ringer's with potassium concentration of 1.0 mEq/l, it appears that values for ε_i and ε_e might be affected by the degree of contraction of the tissue preparation. Therefore, it is recommended that the effects of tension on ε_i and ε_e be studied.

Because experimental data on the membrane potential of vascular smooth muscle cells are very scarce and are not consistent with each other, a value of -57 mV (27) obtained with rabbit ear arteries was employed here for the calculation of the membrane permeability and the active pumping rate. Further research on measuring membrane potentials under various physiological conditions as well as under normal conditions is recommended for the better interpretation of tissue washout data.

Based on the current accumulation of evidence for the electrogenic Na-K pump theory, it is also recommended that washout studies be performed for potassium ion transfer in vascular smooth

muscle to investigate the electrogenicity of the Na-K pump and to obtain the coupling ratio between the sodium and potassium ions being actively transported.

BIBLIOGRAPHY

BIBLIOGRAPHY

1. Anderson, D. K., S. A. Roth, R. A. Brace, D. Radawski, F. J. Haddy and J. B. Scott. Effect of hypokalemia and hypo-magnesemia produced by hemodialysis on skeletal muscle vascular resistance; role of potassium in active hyper-emia. Cir. Res. 31:165, 1972.

2. Arvill, A., B. Johansson and O. Jonsson. Effects of hyper-osmolality on the volume of vascular and smooth muscle cells and the relation between cell volume and muscle activity. Acta. Physiol. Scand. 75:484, 1969.

3. Berman, M. and R. Schoenfeld. Invariants in experimental data on linear kinetics and the formulation of models. J. Appl. Physics 27:1361, 1956.

4. Berman, M., M. Weiss and E. Shahn. Some formal appraoches to the analysis of kinetic data in terms of linear compart-mental systems. Biophys. J. 2:289, 1962.

5. Bohr, D. F. Electrolytes and smooth muscle contraction. Pharm. Rev. 16:85, 1964.

6. Bonting, S. L., K. A. Simon and N. M. Hawkins. Studies on sodium-potassium activated adenosine triphosphatase. I. Quantitative distribution in several tissues of the cat. Arch. Biochem. Biophys. 95:416, 1961.

7. Bozler, E. Conduction, automaticity and tonus of visceral muscles. Experientia 4:213, 1948.

8. Bozler, E. Osmotic phenomena in smooth muscle. Am. J. Physiol. 203:201, 1962.

9. Brace, R. A. and D. K. Anderson. Predicting transient and steady-state changes in resting membrane potential. J. Appl. Physiol. 35:90, 1973.

10. Briggs, A. H. Calcium movements during potassium contracture in isolated rabbit aortic strips. Am. J. Physiol. 203:849, 1962.

11. Briggs, T. Master candidate in the Department of Chemical Engineering, Michigan State University. Personal communi-cation.

12. Burnstock, G. Structure of smooth muscle and its innervation. In Smooth Muscle, ed. by E. Bulbring. Williams & Wilkins, Baltimore, 1970.

13. Burton, C. A. Physiology and biophysics of the circulation. Year Book Medical Publishers, Chicago, 1965.

14. Carnahan, B., H. A. Luther and J. O. Wilkes. Applied numerical methods. Wiley, New York, 1969.

15. Chen, W. T., R. A. Brace, J. B. Scott, D. K. Anderson and F. J. Haddy. The mechanism of the vasodilator action of potassium. Proc. Soc. Exp. Bio. Med. 140:820, 1972.

16. Crank, J. The mathematics of diffusion. Oxford, London, 1956.

17. Daniel, E. E. and M. W. Wolowyk. Electrolyte movements and Na^{22} exchange in vascular smooth muscle. J. Physiol. 214:20p, 1971.

18. Davson, H. and J. F. Danielli. The permeability of natural membrane, 2nd ed. Cambridge Univ. Press, Cambridge, 1952.

19. Dye, J. L. and V. A. Nicely. A general purpose curvefitting program for class and research use. J. Chem. Education 48: 448, 1971.

20. Falk, G. and P. Fatt. Linear electrical properties of striated muscle fibers observed with intracellular electrodes. Proc. Roy. Soc. (London), ser. B, 160:69, 1964.

21. Garrahan, P., M. F. Villamil and J. A. Zadunaisky. Sodium exchange and distribution in the arterial wall. Am. J. Physiol. 209:955, 1965.

22. Geddes, L. A. Electrodes and the measurement of bioelectric events. Wiley, New York, 1972.

23. Goldman, D. E. Potential, impedance and rectification in membranes. J. Gen. Physiol. 27:37, 1943.

24. Hagemeijer, F., G. Rorive and E. Schoffeniels. Exchange of Na^{24} and K^{42} in rat aortic smooth muscle fibers. Life Sci. 4:2141, 1965.

25. Harris, E. J. and G. P. Burn. Transfer of sodium and potassium ions between muscle and the surrounding medium. Trans. Faraday Soc. 46:508, 1949.

26. Headings, V. E., P. A. Rondell and D. F. Bohr. Bound sodium in artery wall. Am. J. Physiol. 199:783, 1960.

27. Hendrickx, H. and R. Casteels. Electrogenic sodium pump in arterial smooth muscle cells. Pflugers Arch. 346:299, 1974.

28. Heppel, L. A. The diffusion of radioactive sodium into the muscle of potassium deprived rats. Am. J. Physiol. 128: 449, 1940.

29. Hodgkin, A. L. and R. D. Keynes. Active transport of cations in giant axons from Sepia and Laligo. J. Physiol. 128:28, 1955.

30. Hodgkin, A. L. and W. A. H. Rushton. The electrical constants of a crustacean nerve fiber. Proc. Roy. Soc. (London), ser. B, 133:444, 1946.

31. Huxley, A. F. Compartmental method of kinetic analysis; appendix 2. In Mineral metabolism: An advanced treatise (C. L. Comar and F. Bronner, eds.), Vol. 1, pt. A, Academic Press, New York, 1960.

32. Jones, A. W. Altered ion transport in large and small arteries from spontaneously hypertensive rats and the influence of calcium. Supplement to Cir. Res. 34-35:117, 1974.

33. Jones, A. W. and G. Karreman. Ion exchange properties of the canine carotid artery. Biophys. J. 9:884, 1969.

34. Jones, A. W. and M. L. Swain. Chemical and kinetic analysis of sodium distribution in canine lingural artery. Am. J. Physiol. 223:1110, 1972.

35. Keynes, R. D. The ionic fluxes in frog muscle. Proc. Roy. Soc. (London), ser. B, 142:359, 1954.

36. Keynes, R. D. The energy source for active transport in nerve and muscle. In Membrane transport and metabolism (A. Kleinzeller and A. Kotyk, eds.), Academic Press, New York, 1961.

37. Ling, G. N. A physical theory of the living state. Blaisdell Publishing Co., Waltham, 1962.

38. Ling, G. N. Cell membrane and cell permeability. Ann. N.Y. Acad. Sci. 137:837, 1966.

39. Llaurado, J. G. Special communications: Digital computer simulation as an aid to the study of arterial wall Na kinetics. J. Appl. Physiol. 27:544, 1969.

40. Llaurado, J. G. Some effects of aldosterone on sodium transport rate constants in isolated arterial wall: Studies with computer simulation and analysis. Endocrinology 87: 517, 1970.

41. Lullman, H. Calcium fluxes and calcium distribution in smooth muscle. In Smooth muscle (E. Bulbring, ed.), Williams & Wilkins, Baltimore, 1970.

42. Maizels, M. Factors in the active transport of cations. J. Physiol. 112:59, 1951.

43. Panner, B. J. and C. R. Honig. Filament ultrastructure and organization in vertebrate smooth muscle. J. Cell Biol. 35:303, 1967.

44. Pikal, J. M. Diaphragm cell diffusion studies with short prediffusion times. J. Phys. Chem. 74:4165, 1970.

45. Plonsey, R. Bioelectric phenomena. McGraw-Hill, New York, 1969.

46. Potter, J. M. and M. P. Sparrow. The relationship between calcium content of depolarized mammalian smooth muscle and its contractility in response to acetylcholine. Aust. J. Exp. Biol. Med. Sci. 46:435, 1964.

47. Robertson, J. D. Unit membranes: A review with recent new studies of experimental alterations and a new subunit structure in synoptic membranes. In Cellular membranes in development (M. Locke, ed.), Academic Press, New York, 1964.

48. Robertson, J. S. Theory and use of tracers in determining transfer rates in biological systems. Physiol. Rev. 37:133, 1957.

49. Scott, J. B., R. M. Daugherty, Jr., H. W. Overbeck and F. J. Haddy. Vascular effects of ions. Fed. Proc. 27:1403, 1968.

50. Skou, J. C. Further investigations on a Mg^{++} + Na^+-activated adenosine-triphosphatase, possibly related to the active, linked transport of Na^+ and K^+ across the nerve membrane. Biochem. Biophys. Acta. 42:6, 1960.

51. Skou, J. C. Enzymatic basis for active transport of Na^+ and K^+ across cell membrane. Physiol. Rev. 45:596, 1965.

52. Somlyo, A. P. and A. V. Somlyo. Vascular smooth muscle. Pharm. Rev. 20:197, 1968.

53. Somlyo, A. V. and A. P. Somlyo. Electromechanical and pharm-arcomechanical coupling in vascular smooth muscle. J. Pharmac. Exp. Ther. 159:129, 1968.

54. Su, C., J. A. Bevan and R. C. Ursillo. Electrical quiescence of pulmonary artery smooth muscle during sympathomimetic stimulation. Cir. Res. 15:20, 1964.

55. Thomas, R. C. Electrogenic sodium pump in nerve and muscle cells. Physiol. Rev. 52:563, 1972.

56. Villamil, M. F., V. Retori, L. Barajas and C. R. Kleeman. Extracellular space and the ionic distribution in the iso-lated arterial wall. Am. J. Physiol. 214:1104, 1968.

57. Waugh, W. H. Adrenergic stimulation of depolarized arterial muscle. Cir. Res. 11:264, 1962.

58. Wolowyk, M. W., A. M. Kidwai and E. E. Daniel. Sodium-potassium stimulated adenosinetriphosphatase of vascular smooth muscle. Can. J. Biochem. 49:376, 1971.

59. Zelman, A. and H. H. Shih. The constant field approximation: numerical evaluation for monovalent ions migrating across a homogeneous membrane. Biophys. Soc. Absts., p. 214, 1972.